Technoeconomic Optimization of a Conceptual Flowsheet for Continuous Separation of an Analgaesic Active Pharmaceutical Ingredient (API)

Technoeconomic optimisation of a conceptual flowsheet for continuous separation of an analgaesic Active Pharmaceutical Ingredient (API)

Hikaru G. Jolliffe and Dimitrios I. Gerogiorgis*

Institute for Materials and Processes (IMP), School of Engineering, University of Edinburgh, The King's Buildings, Edinburgh, EH9 3JL, United Kingdom

**Corresponding author: D.Gerogiorgis@ed.ac.uk (+44 131 6517072)*

ABSTRACT

Continuous Pharmaceutical Manufacturing (CPM) has recently emerged as a promising alternative to current batch production methods which are plagued by issues of product quality, process reliability and cost. With advances in new continuous synthesis routes, demonstrations of full end-to-end continuous drug production and comparative analyses explicitly showing its advantages, CPM has been attracting interest at the highest levels of industry and regulators. While continuous chemistry has been demonstrated for a variety of Active Pharmaceutical Ingredients (APIs), and there have been a few some landmark studies demonstrating practical CPM covering a full design from raw materials to final product formulation, fully continuous separation, critical to maximising full CPM potential, remains to be fully elucidated.

In this work we formulate a nonlinear optimisation problem for the CPM of ibuprofen. Adapting published continuous synthesis routes and experimental data, and considering reactor design, explicit mass transfer, thermodynamics via UNIFAC-estimated API solubilities, and cost estimation, optimal total costs were determined for two solvents, toluene and n-hexane, for three different temperature cases, 25 °C, 45 °C, and 65 °C.

A lowest total cost (728.5×10^3 GBP) is achieved for n-hexane use at 65 °C. The best total cost for toluene is only marginally higher (761.4×10^3 GBP, also at 65 °C). With respect to the E-factor, a measure of design sustainability, the cases are comparable: the best E-factor (39.9) is for the n-hexane at 65 °C, and the best E-factor for toluene is again close at 42.1 (for 65 °C). Given that the differences are small, the use of toluene at 65 °C is the preferable option, as it is more benign than n-hexane.

1 INTRODUCTION

Financial, technical and market pressures on the pharmaceutical industry (Figure 1) have led to the emergence of Continuous Pharmaceutical Manufacturing (CPM) as a promising alternative to current batch production methods.[1] While batch process have advantages including equipment flexibility and the ability to recall specific batches, they nevertheless have issues with product quality, process reliability and cost;[2] as a mature technology, batch process improvements are also incremental at best. With advances in new continuous synthesis routes, demonstrations of full end-to-end continuous drug production and comparative analyses explicitly showing its advantages, CPM has attracted interest at the highest levels of industry and regulators.[3,4]

The foundation of any CPM process is the continuous chemistry, and this was demonstrated for a variety of APIs from common painkillers to blockbuster anti-cancer medications, as well as key substances in the fight against debilitating tropical diseases.[6–8] Toward demonstrating practical CPM, some landmark studies cover a full design from raw materials to final product formulation.[9] However, fully continuous separation, critical to maximising full CPM potential, remains to be fully elucidated; significant research is being conducted in this field.[10]

Process modelling, simulation and cost estimation are rapid and low-cost methodologies for evaluating the benefits of continuous processing for the production of pharmaceuticals,[1,11–12] while optimisation, also called mathematical programming, is a vibrant field with many applications.[13–15] It has been applied to many aspects of pharmaceuticals and CPM.

A typical example by Grom et al.[16] investigated the reaction kinetics, pathways and process optimisation of Lorcaserin, a weight-loss drug belonging to the benzazepine class of heterocyclic compounds. The complex kinetics, with over 15 species, 27 reactions, and 29 parameters to be optimised, were formulated into a nonlinear regression problem using the Levenberg-Marquadt algorithm. The efficient formulation allowed a global optimum to be reached while significantly reducing the number of initial approximations required. The model developed allowed the optimal process conditions (temperature, reaction time, concentrations) to be found.

Optimal reactor and process design for the small-scale implementation of continuous ibuprofen synthesis – the chemistry for which was developed by Bogdan et al.[6] – was studied by Patel et al.[17]. This work focused purely on the specific design and operation of a microreactor (mass and energy balances, reaction rates, reactor configuration, the partial differential equations of which were discretised) without considering product separation or process economics. The optimisation problem, which included 67 degrees of freedom, was formulated as a minimisation of the difference between heat removed from and heat generated by the microreactor assembly in order to achieve optimal

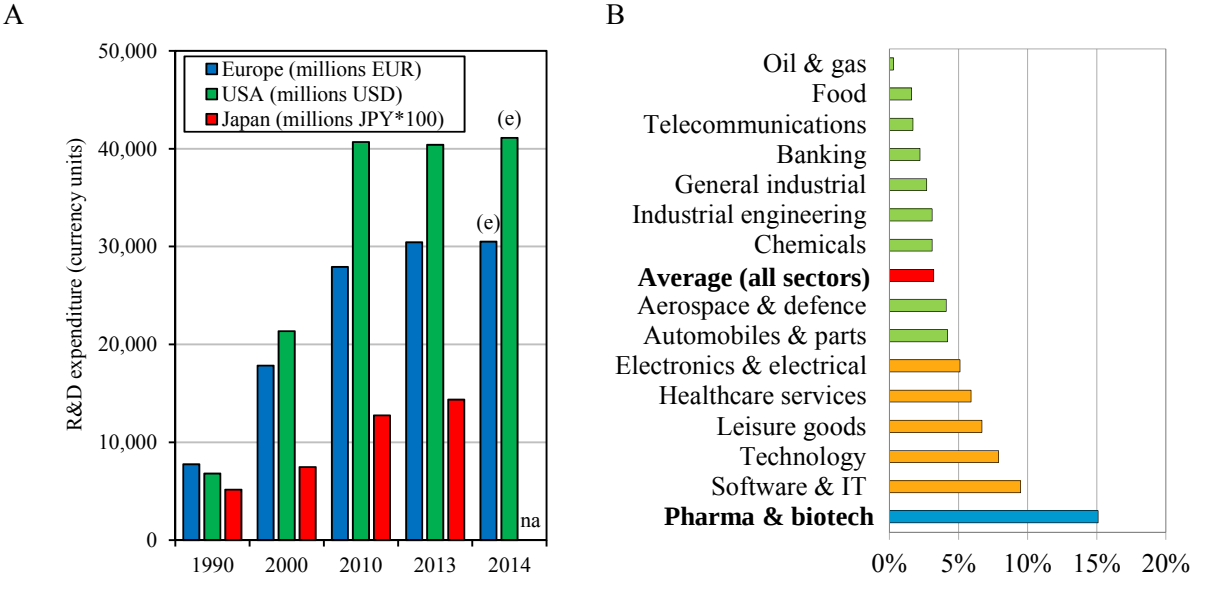

Figure 1. Economic and market pressures faced by the pharmaceutical industry. A: typical R&D sector expenditure.[5] B: industry sector R&D costs as a percentage of net sales.[5]

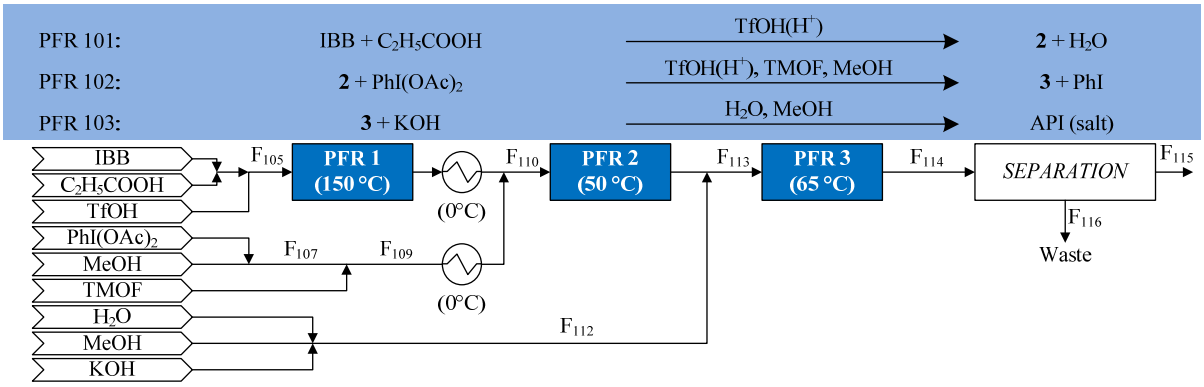

Figure 2. Demonstrated process flowsheets for ibuprofen CPM.[6]

configuration and operating conditions; constraints and bounds included residence times, temperature, and concentrations. The results underlie the utility of such investigations of reactor and process design toward informing robust and sustainable process options.

CPM process life-cycle assessments are also excellent candidates for optimisation. By systematically considering a diverse set of sustainability metrics such as Process Mass Intensity, Cumulative Energy Demand and E-factor in addition to technical parameters. Ott and co-workers[18,19] showed how several routes for rufinamide (an anti-convulsant) synthesis can be compared in a meaningful way, elucidating their comparative impacts on the environment, and reducing the LCIA (Life Cycle Impact Assessments, another environmental impact metric) by up to 45 %.

There is also vibrant research investigating the optimisation and control of continuous separation and downstream product formulation processes.[20-23] Boukouvala and Ierapetritou used surrogate-based optimisation to reduce the computational cost of complex solid-based flowsheet models, using deterministic Kriging and with added noise;[20] the process model used in this case was also used for simulations.[11,24] The work combines well known simulation-optimization concepts with black-box feasibility analyses and heteroscedastic data regression, toward the optimization of computationally expensive process. While the authors acknowledged that the approach does not encapsulate all possible sources of variability, it offered good potential for refinement and further development, and the added benefit of such approaches will be higher for process of greater inherent complexity.[20] In contrast to the surrogate approach, others have explicitly optimized an integrated downstream

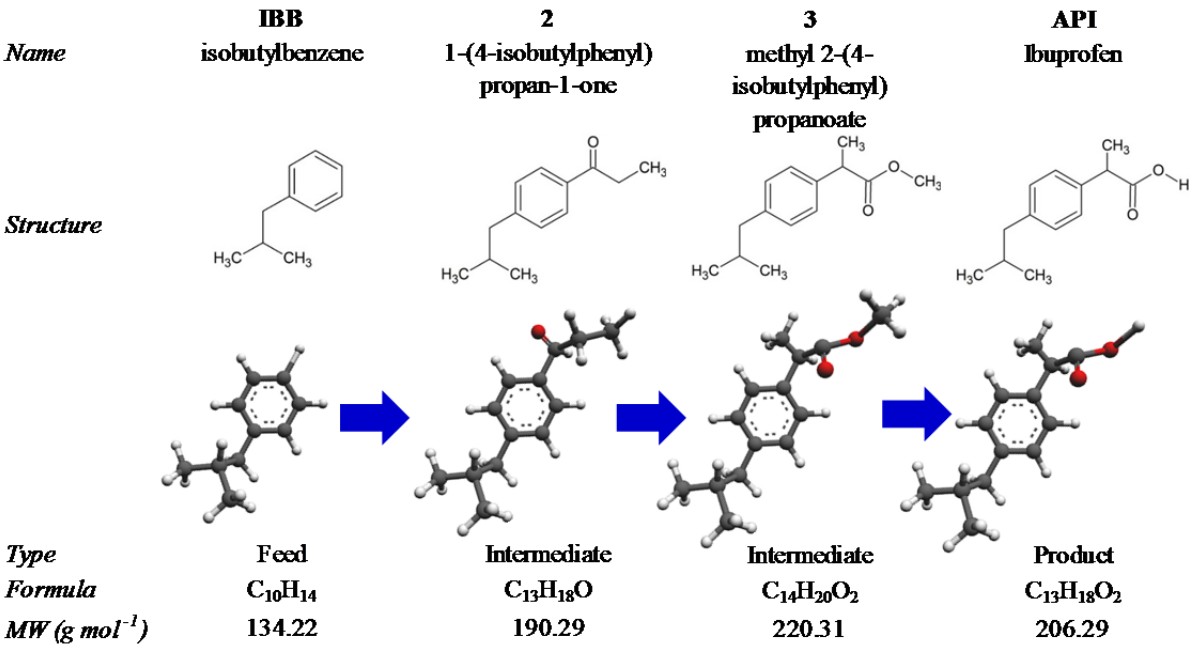

Figure 3. Reaction sequence used by Bogdan et al.[6] for continuous ibuprofen synthesis.[6]

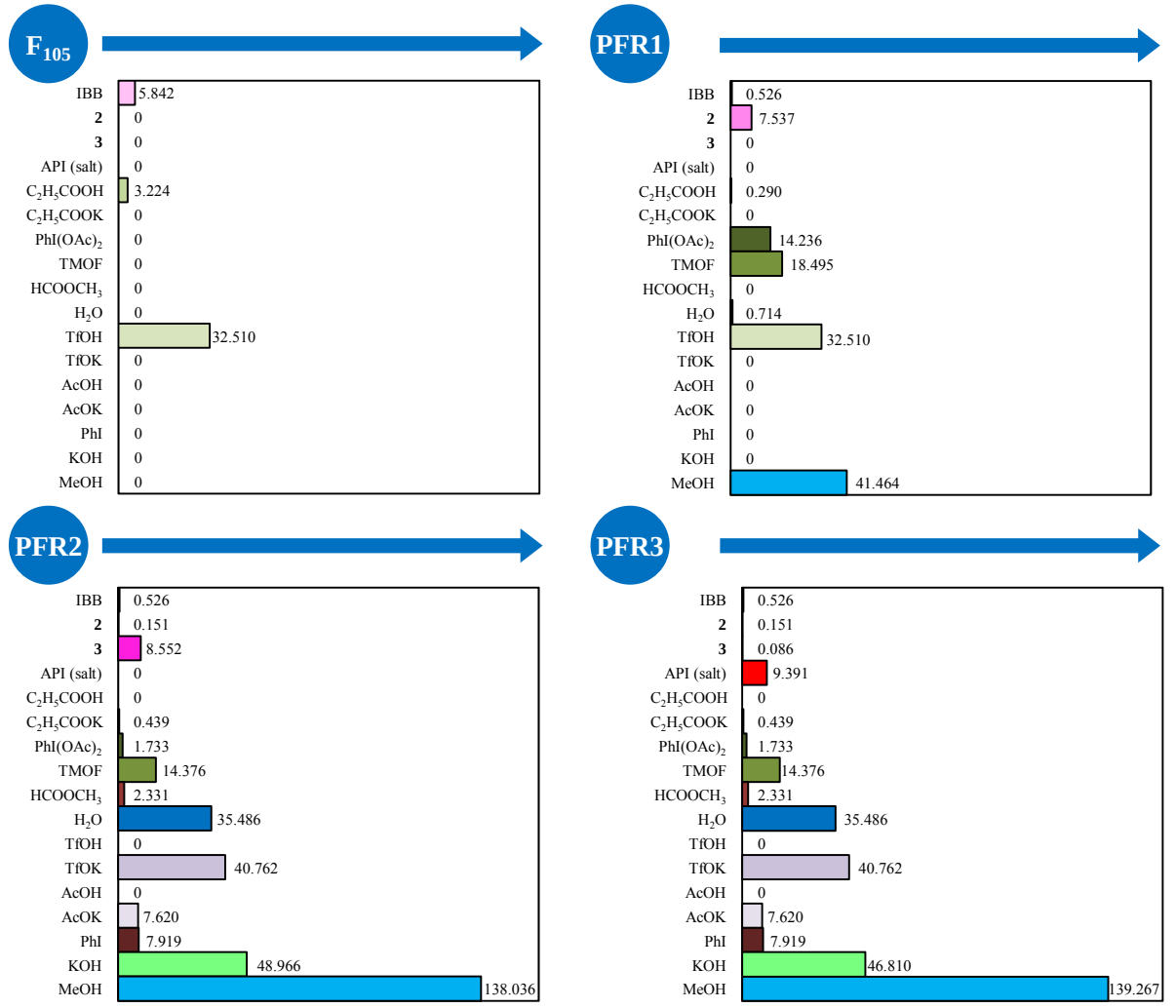

Figure 4. Continuous ibuprofen synthesis mass balance at key flowsheet points [25].

flowsheet comprising crystallisation, filtration, drying and mixing;[21] for the latter there is the noteworthy joint use of reduced-order models for particle velocity prediction coupled with population balance models for macroscopic property quantification. Separate objective functions for each unit operation, optimizing respective aspects of design or operation (e.g. maximizing crystal growth, maximizing filtration rate, minimization in deviation from expected final API content specification) employed, with robust results; a built-in solver of gPROMS was used, which follows a sequential quadratic programming algorithm.[21] Abejón et al.[22] investigated the optimization of a complex nanofiltration cascade, with the objective of minimizing the total cost. They considered process modelling, unit configuration and economic evaluation. The resulting nonlinear optimization problem was solved using the GAMS software package, via the use of Pareto diagrams to help identify ideal scenarios, and with the additional inclusion of solvent recovery operations, it was found that total costs could be reduced by up to 77%.

In this present work, we present the optimisation of a conceptual upstream flowsheet with product Active Pharmaceutical Ingredient (API) recovery: a nonlinear optimisation model is formulated to maximise the design Net Present Value/NPV. An explicit model of the entire flowsheet using deterministic optimisation, the cost function firstly depends on the economic considerations of revenue, operating expenditure (OpEx), and fixed capital expenditure (CapEx), as well as design lifetime and rate of inflation. Revenue is determined by the rate of product API recovery from final separation. This in turn is determined by technical aspects of the flowsheet, the primary components of which are three continuous plug flow reactors with subsequent separation and product recovery. The flowsheet is an expanded, more detailed design of previous efforts.[25]

We also investigate continuous separation schemes to replace a 15-step batch process for final product recovery. A range of possible options for continuous separation are included in the model via equations governing product recovery and separation: this includes UNIFAC estimation of API solubility in a selection of possible 'green' solvents (those of lowest toxicity and environmental impact, including ethanol, ethyl acetate and acetonitrile) and process operating parameters (e.g. temperature, solvent ratio). This is followed by the minimization of total cost by nonlinear optimisation on the basis of a detailed continuous process model, where constraints include product purity and sustainability (via waste limitation) in addition to technical considerations, before concluding some key remarks for optimal CPM process design.

The scope of this paper builds upon the success of several (academic but also corporate) studies[6-10] which consider continuous flow syntheses and demonstrate original CPM plant implementations; the production-scale technical efficiency[25,28] and economic viability[29,36] of the latter remain to be analysed, but it is also critical to hereby evaluate relative CPM solvent performance. The frequent scarcity of public-domain kinetics is exacerbated by the dire need for mass transfer efficiency data; if this is not essential in batch pharma operations (where equilibrium assumptions may be plausible), it is a fundamental necessity in continuous manufacturing, where mass transfer is of critical importance. We thus explicitly consider thermodynamics as well as mass transfer efficiency in LLE design, in order to perform economic NLP optimisation under a realistic, suitably detailed CPM process model.

2 PROCESS FLOWSHEET AND CONTINUOUS PRODUCT SEPARATION

Ibuprofen is a widely used, essential painkiller with significant market presence. The first widely implemented industrial synthesis method has generally been replaced by a more efficient and simpler route. The group of [6] recently synthesised ibuprofen using novel continuous chemistry in a landmark study (Figure 2, Figure 3). We have previously performed initial technoeconomic evaluations of ibuprofen – using the work of Bogdan et al.[6] as a foundation – and also for a key antimalarial API.[25,28] This work here is an extension of our efforts with regards to ibuprofen.

	PFR 1	PFR 2	PFR 3
Reaction	1	2	3
Reaction order	2	2	2
Reaction type	Friedel-Crafts acylation	1,2-aryl migration	Base hydrolysis
Rate law	$-r_{IBB} = k_1 C_{IBB} C_{C_2H_5COOH}$	$-r_2 = k_2 C_2 C_{PhI(OAc)_2}$	$-r_3 = k' C_3$
Reactor temperature (°C)	150	50	65
Conversion (%)	91	98	99
Rate constant k_i (L mol^{-1} hr^{-1})	31.41	2732.3	15.57
Coefficient of determination (R^2)	0.836	0.978	–
Method for k_i	Data analysis	Data analysis	SPARC model[26,27]

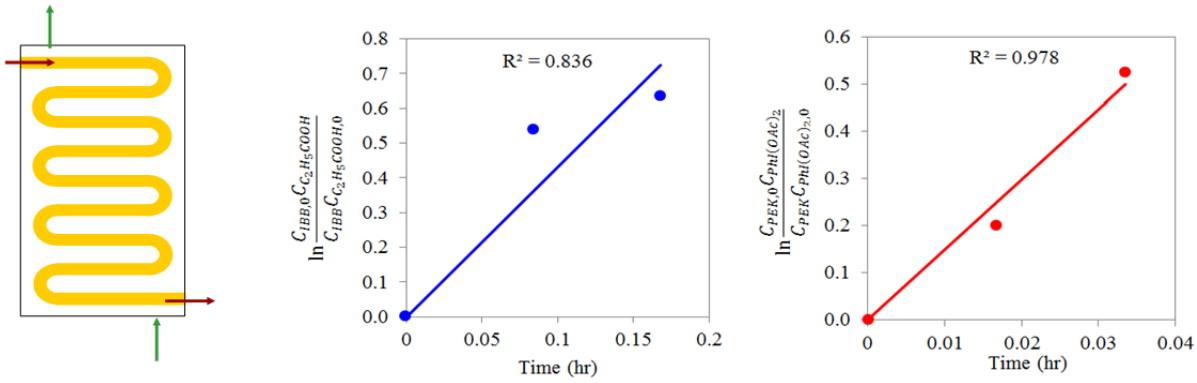

Figure 5. Kinetic data analysis for reactor design.[6,25]

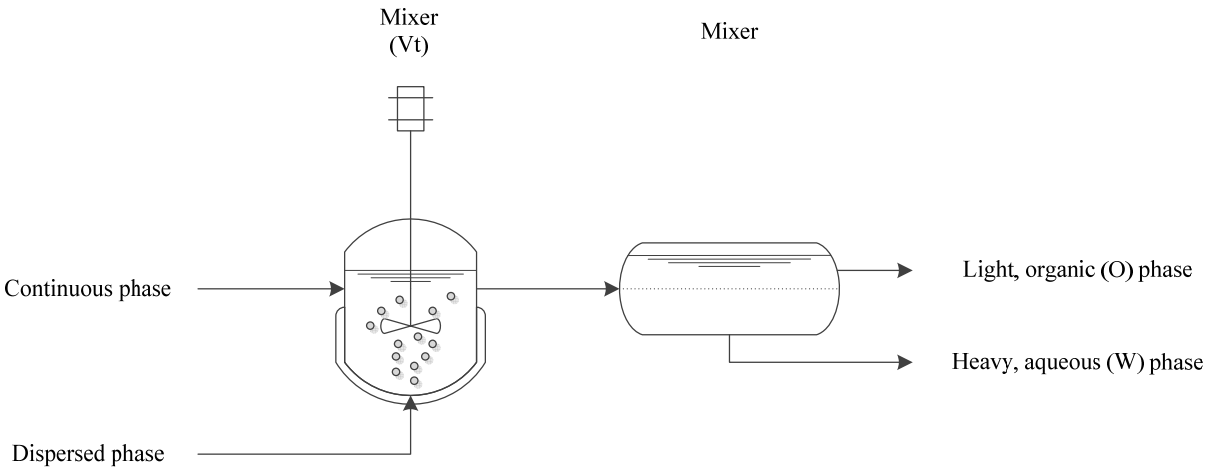

Figure 6. Ibuprofen product recovery: conceptual continuous purification scheme.

2.1 Reaction scheme

The ibuprofen process flowsheet studied in this work is based on the publication of Bogdan et al.[6] (Figure 2). Three plug flow rectors (PFRs) in sequence are employed, because of the high yield which is achieved in many similar continuous flow synthesis routes, as documented in recent studies[4, 6-10]; an example mass balance (for the same process at a different scale) is given in Figure 4. The equations governing the chemical reactions in each reactor are formulated with reaction order and rate constants determined from kinetic data analysis of the publication by Bogdan et al.[6]. In the first PFR, operating at 150 °C, the key ingredient isobutyl benzene (IBB) reacts with propanoic acid in a Friedel-Crafts acylation reaction, where the solvent is neat triflic acid (TfOH), which also acts as an acid catalyst. A conversion of 91% is achieved, producing the intermediate molecule **2**, 1-(4-isobutylphenyl)propan-1-one; the reactor effluent is then chilled to 0°C and mixed with additional reagents and solvents that have also been chilled, before progressing to the next PFR.[6]

In the second reactor (operating at 50°C) a diacetoxyiodobenzene-mediated 1,2-aryl migration reaction transforms intermediate **2** to 2-(4-isobutylphenyl)propanoate, or intermediate **3**, at 98% conversion. The reactor effluent is combined with a binary water-methanol stream containing potassium hydroxide – neutralising the acid – and the resulting mixture enters the third and final reactor.

The saponification of **3** occurs in the third reactor, which operates at 65°C, producing ibuprofen in the potassium salt form. This is re-acidified with strong acid – reverting ibuprofen to a carboxylic acid – during product purification and recovery.[6]

2.2 Continuous API product separation

Continuous separation alternatives have significant promise in delivering cost and sustainability benefits, and here we model two continuous liquid-liquid extraction options we have previously reported, using updated modelling tools.[25,27,28] The first option uses toluene as a waste-extracting solvent, while the second uses n-hexane. The former has the advantages of lower environmental impact (toluene is less toxic and damaging than n-hexane), while n-hexane can offer better performance in terms of product recovery. Toluene use is normally recommended here; nevertheless, n-hexane use is analysed in order to determine the difference in costs. An example flowsheet of this separation process is given in Figure 6. After base neutralisation with acid, the resulting acidified stream then proceeds to a liquid-liquid extraction operation, where either toluene or n-hexane is used.

Our essential focus here is designing a continuous liquid-liquid extraction (LLE) vessel, modelled as a small mixer-settler, where the mixer is a continuous stirred tank. The reason a continuously stirred separation tank (similar to a CSTR) is considered here is the potential to ensure (but also manipulate the stirring power toward) a high interfacial area between the aqueous and organic phases, which in turn greatly facilitates rapid API mass transfer (continuous plug flow separators have also

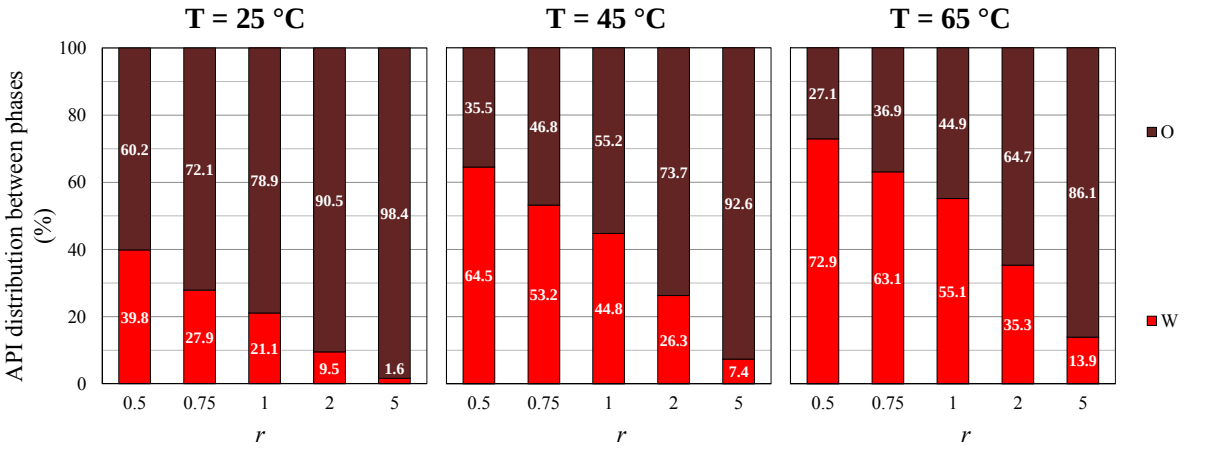

Figure 7. Theoretical API distribution between product aqueous (W) and waste organic (O) phases as a function of the solvent-to-feed mass ratio (r), using toluene as the LLE solvent.

been demonstrated in the literature, but without control of the interfacial area available for mass transfer).[40] We consider two distinct liquid-liquid extraction (LLE) solvents (toluene and n-hexane) and three distinct temperatures of ambient (25 °C), and intermediate temperature (45 °C) or the temperature which coincides with the effluent of the third PFR (65 °C); we employ the UNIFAC solubility estimation for computing ibuprofen solubilities.

Initial investigations of API solubility in a ternary mixture of methanol (the process solvent), water (present in significant quantities) and the separation solvent (toluene or n-hexane) illustrate varying performance with temperature and rate of separation solvent use. This is illustrated in Figure 7 (toluene) and Figure 8 (n-hexane), which shows the percentage of API in either the organic or aqueous phases that result from the ternary mixture.

3 NONLINEAR OPTIMISATION PROBLEM

The formal posing and mathematical formulation of the total cost minimisation considers a sum of capital as well as time-discounted operating expenditure. The cost was calculated as the sum required to purchase, build and run a given design for a specified time period:

$$\min NPV = CapEx + \sum_{t=1}^{\tau} \left\{ \frac{OpEx}{(1+y)^t} \right\} \tag{1}$$

s.t.

$$CapEx = BLIC + C_{cont} + C_{wc} \tag{2}$$

$$OpEx = C_{mat} + C_{utl} + C_{was} \tag{3}$$

where the total cost is represented by the Net Present Value, and τ is the design lifetime (20 years), and y is the discount rate to the present day (5 %); these are conservative estimates of the economic climate and plant longevity, and similar values have been used in previous publications.[1, 29, 36] *CapEx* is the capital expenditure (consisting of the Battery-Limits Installed Cost, *BLIC*, cost of contingency C_{cont}, and working capital, C_{WC}) and *OpEx* is the operating expenditure (consisting of the cost of material purchase, C_{mat}, utilities (C_{util}) and waste disposal, C_{waste}).
Further equations involved in the computing the terms in equations (2-(3) are detailed below.

3.1 Process modelling

The three plug flow reactors have been simulated using the standard performance equation for a second-order reactions:

$$V_{PFRm} = \frac{\dot{Q}_m C_{mi0}}{k_i} \int_0^{X_{mif}} \frac{dX_{mi}}{(C_{mi0} - C_{mi0} X_{mi})(C_{mj0} - C_{mj0} X_{mi})} \tag{4}$$

where V_{PFRm} is the volume of reactor m, $\dot{Q}_m$ is the volumetric flowrate through m, subscripts i and j respectively denote reactant species i and j (species i being the one for which reaction data was available), k_i is the reaction rate constant, and X is conversion.

For the three reactions that occur here, one in each reactor, rate constant values have been determined from systematic evaluation of published kinetic data, while for the last reaction a predictive model was used (Figure 5). It should be noted that we are not optimising over the operating temperature of the three respective reactors, as we do not have the requisite data to derive explicit Arrhenius kinetics. Further details can be found in the publication by.[25] The values used are reliable, and correspond to the operating temperatures of the reactions. Computed reactor volumes are used to estimate their cost.

To avoid overcomplicating the model (including avoiding explicit UNIFAC equations in the model, which could significantly increase computational demand) we have pre-processed and obtained a set of data from extensive simulations on the basis of UNIFAC method and derived surrogate equations;[31] the average R^2 value for surrogate equations used in this work is over 0.99.

These have been fitted with either geometric or polynomial functions in order and incorporated into the NLP model that we have solved.

The liquid-liquid-extractor (LLE) was modelled as a mixer-settler. To compute the ternary mole fractions of the two liquid phases (organic and aqueous) in the mixer, surrogate equations were used (Figure 9):

$$x_{ipsT} = A_{ipsT} r^2 + B_{ipsT} r + C_{ipsT} \tag{5}$$

where x is mole fraction; subscript p refers to phase (organic or aqueous), s refers to solvent used (toluene or n-hexane), and T is temperature (25°C, 45 °C, or 65°C); A, B and C are coefficients; and r is the ratio of solvent s to incoming feed stream (by mass).

The theoretical maximum API recovery is also computed from high-fidelity surrogate equations (Figure 10):

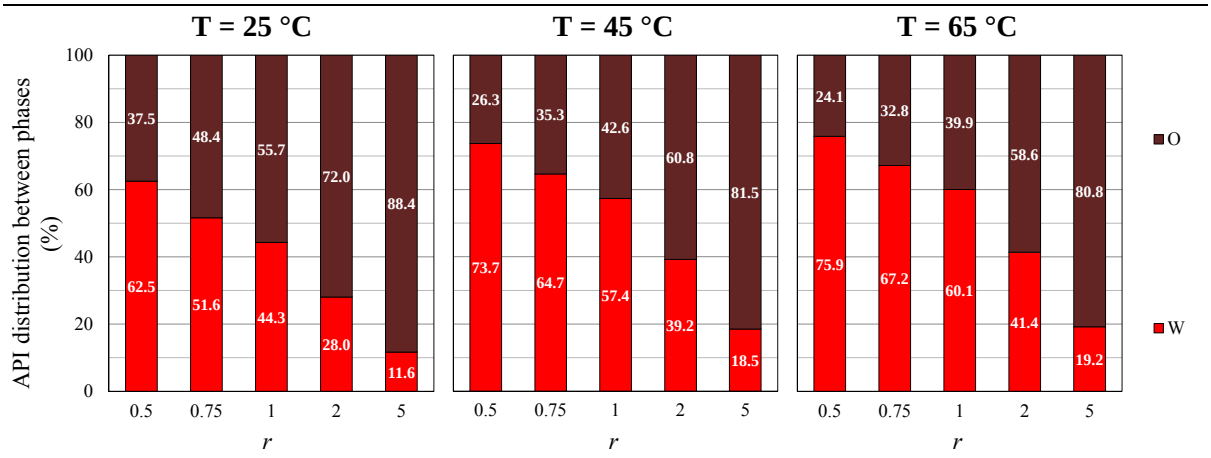

Figure 8. Theoretical API distribution between product aqueous (W) and waste organic (O) phases as a function of the solvent-to-feed mass ratio (r), using n-hexane as the LLE solvent.

$$R_{max,sT} = A'_{sT} e^{B'_{sT} r} \tag{6}$$

To calculate the concentration of ibuprofen in the product stream exiting the mixer, the stage efficiency was computed:

$$E_{sT} = \frac{1}{\left(\frac{\dot{Q}_{sT}}{K_{sT} a_{sT} V_{tsT}} \right) + 1} \tag{7}$$

where $\dot{Q}_s$ is the volumetric flow through the LLE tank, K is the overall mass-transfer coefficient, a is the interfacial area, and V_t is LLE tank volume; other subscripts are as previously described. The rate of API recovery is then calculated as follows;

$$\dot{f}_{sT} = K_{sT} a_{st} \left(C^*_{sTd} - C_{sTd} \right) \tag{8}$$

where, C^*_{sTd} is the equilibrium API concentration in the dispersed phase in the mixer, calculated using the maximum theoretical API recovery R_{max}, while C_{sTd} is the operating concentration (also that of the product stream), which is calculated using the stage efficiency $E_{s,T}$.

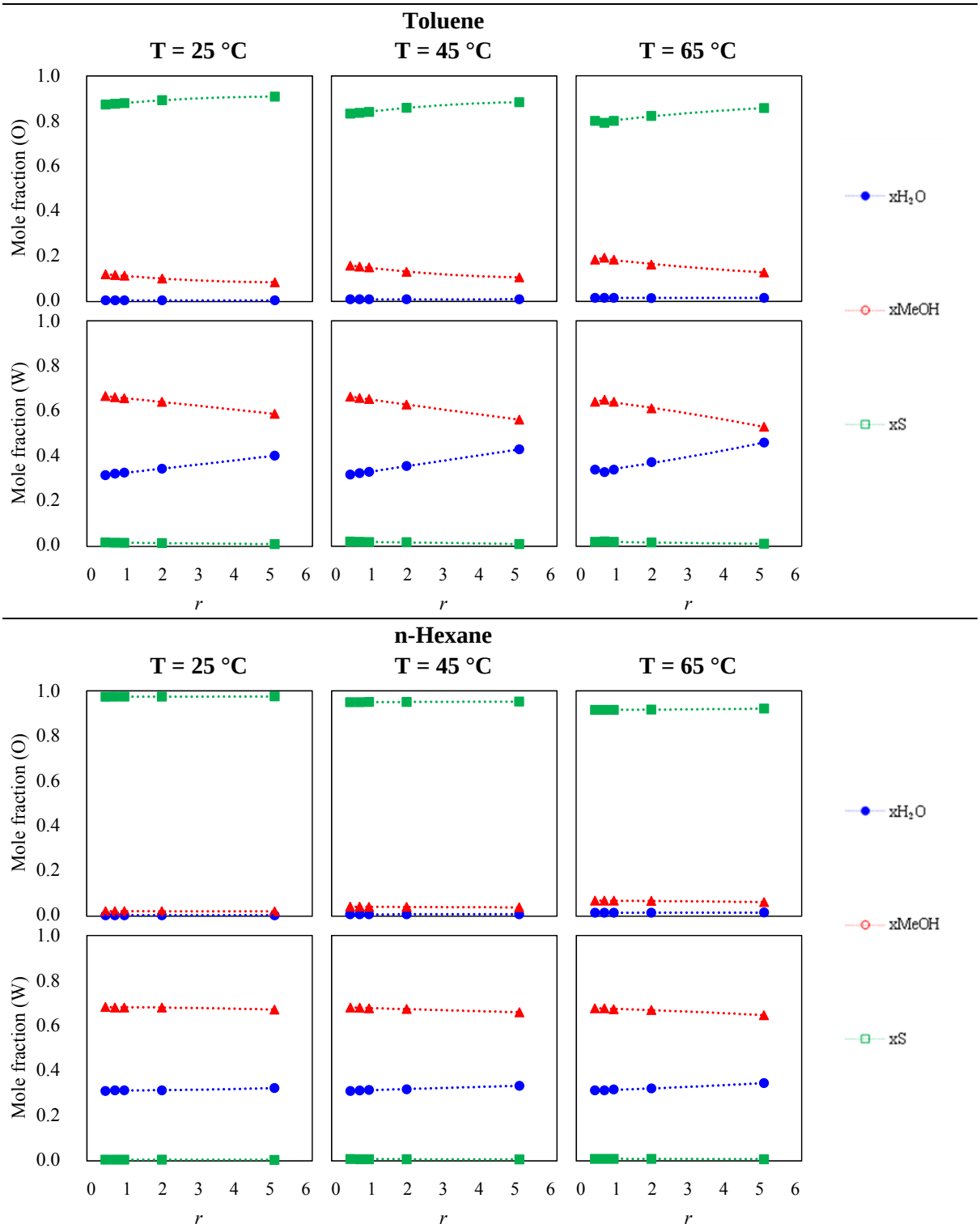

Figure 9. Determination of surrogate mole fraction equations for water (xH_2O), methanol (xMeOH) and LLE solvent (xS) ternary phase (organic, O, or aqueous, W) varying by solvent-to-feed ratio *r*. Surrogate equations are fitted second-order polynomials with $R^2 > 0.96$.

In order to compute the overall mass-transfer coefficient *K*, dispersed (subscript *d*) and continuous (subscript *c*) phase mass-transfer coefficients were computed using the correlation developed by Skelland and Moeti:[32]

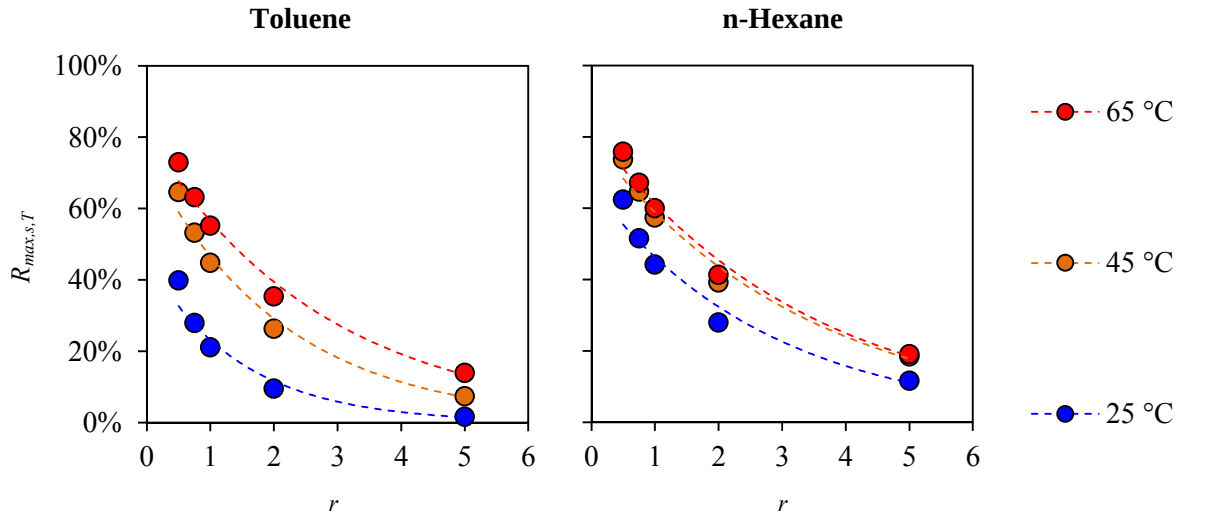

Figure 10. Surrogate equations maximum theoretical product recovery ($R_{max,sT}$) in the LLE aqueous (W) phase, varying by solvent-to-feed ratio *r*. Surrogate equations are fitted exponential functions with $R^2 > 0.96$.

$$K = \frac{1}{\frac{1}{k_c} + \frac{1}{k_d}} \tag{9}$$

$$Sh_d = \frac{k_d d_{32}}{D_{API,d}} = 6.6 \tag{10}$$

$$Sh_c = \frac{k_c d_{32}}{D_{API,c}} = 1.27 \times 10^{-5} Sc_c^{1/3} Fr_c^{5/12} Eo^{5/4} \varphi^{-1/2} Re_i^{2/3} \left(\frac{d_i}{d_{32}}\right)^2 \left(\frac{d_{32}}{d_t}\right)^{1/2} \tag{11}$$

where *Sh* are Sherwood numbers, k_d and k_c the phase-specific mass transfer coefficients, d_{32} is the Sauter mean droplet diameter of the dispersed phase, D_{API} is the diffusivity of ibuprofen in the phases, *Sc* is the Schmidt number, *Fr* the Froude number, *Eo* the Eotvos number, φ the dispersed phase volume fraction, Re_i the impeller Reynolds number, d_i the impeller diameter and d_t the tank internal diameter:

$$Sc_c = \frac{\mu_c}{\rho_c D_{API,c}} \tag{12}$$

$$Fr_c = \frac{d_i N_i^2}{g} \tag{13}$$

$$Eo = \frac{\rho_d d_{32}^2 g}{\sigma} \tag{14}$$

$$Re_i = \frac{d_i^2 N_i \rho_m}{\mu_m} \tag{15}$$

$$D_{API,p} = \frac{k_b T}{6\pi\mu_p r_{API}} \tag{16}$$

where μ is viscosity; ρ is density; σ is surface tension; N_i is impeller rotation speed; *g* is gravity; V_d and A_d are dispersed phase droplet volume and area, respectively; and r_{API} is the molecular radius of ibuprofen. As before, subscripts *c* and *d* refer to the continuous and dispersed phases, while subscript *p* can be either. The Sauter mean droplet diameter, d_{32}, is calculated from the Weber number (*We*), depending on the magnitude of the latter, and there is a maximum permissible size for d_{32} (10^{-3} m):

$$d_{32} = \begin{Bmatrix} 0.052 d_i We^{-0.6} e^{4\varphi} & ,We < 10^3 \\ 0.39 d_i We^{-0.6} & ,We > 10^3 \end{Bmatrix} \quad (17)$$

$$We = \frac{d_i^3 N_i^2 \rho_c}{\sigma} \quad (18)$$

The specific interfacial area a is computed form the dispersed phase volume fraction and the Sauter mean droplet diameter:

$$a = \frac{6\varphi}{d_{32}} \quad (19)$$

The LLE tank itself was assumed to have a height : diameter ratio of 1, a tank : impeller ratio of 2, and an impeller rotation speed of 6 rps.

3.2 Cost estimation

The calculations assume that the design will be constructed onsite at an existing pharmaceutical facility; a 335-day working year (8,040 hours) was assumed. A variety of vendor data and established economic prediction methods were used to estimate both Capital Expenditure (CapEx) and Operating Expenditure (OpEx). Where possible, vendor prices were used for process equipment of comparable capacity, and capacity-cost correlations were used this data unavailable.[33]

The CapEx (2) includes the Battery Limits Installed Cost (*BLIC*), contingency (C_{cont}) and working capital (C_{WC}):

$$BLIC = FOB_{tot} C_{ins} (1 + C_{pip} + C_{ins\,2})(1 + C_{ec}) \quad (20)$$

$$FOB_{Tot} = \sum_i \left(n_i C_{ai} \left(\frac{S_{bi}}{S_{ai}} \right)^{p_i} cf_i \right) \quad (21)$$

$$C_{con} = f_{con} BLIC \quad (22)$$

$$C_{wc} = f_{wc} C_{mat} \quad (23)$$

Subscripts B and A denote two identical pieces of equipment which are at different scales, or capacities, given by S_B and S_A. These capacities are of a dimension inherent to the equipment: examples include tank volume and filter area. The exponent n is particular to a type of equipment, and typically ranges between 0.0–1.0. In addition, other factors, summarised above as f can be applied to take into account design options such as construction material or design operating conditions. Where there is a significant surplus in the applicable capacity range to the required capacity, these additional factors were not used. Where the determined price corresponds to the past, the Chemical Engineering Plant Cost Index (CEPCI) was used to calculate the inflation to allow appropriate cost adjustments to the present time.

The use of inflation-adjusted equation (21) produces the Free-on-Board (FOB) cost. The Chilton Method was then used to estimate the Battery-Limits-Installed-Cost.[34] The installed equipment cost C_{ins} was taken to be 1.43 times the FOB. Process piping C_{pip} and instrumentation C_{ins2}were taken to be 0.3 and 0.12 times the installed equipment costs, respectively; the sum of the installed, piping, and instrumentation costs then forms the total physical plant cost, to which a final factor for engineering and construction C_{ec} (0.3) is included, producing the BLIC.

The working capital C_{wc} is estimated to be 3.5% of annual material costs.[1] The contingency C_{con} was set at 20% of the BLIC. Finally, the total CapEx required is then the sum of the BLIC and the WCC.

The cost of material purchase (C_{mat}, including reagents, catalysts and solvents) forms a significant portion of the OpEx, equation (3); the rest includes utilities (C_{utl}) and waste disposal (C_{was}) costs:

$$C_{mat} = \sum_j Req_j C_{purc,j} \tag{24}$$

$$C_{utl} = f_{utl} \sum_j Req_j \tag{25}$$

$$C_{was} = f_{was} \dot{v}_{was} \tag{26}$$

The vast majority of waste is solvent and antisolvent, and as such these have been assumed to be the entirety of the waste with respect to calculating waste handling costs.

The material prices have been sourced from vendors as well as official records of imports and exports to and from countries including but not limited to France, Spain, Germany, Iran, Saudi Arabia, China, Bangladesh and India.

A subset of the established heuristics employed by Schaber et al.[1] have been used to estimate the balance of the OpEx, which is utilities and waste disposal costs. Utilities costs have been estimated based on the total amount of material input: a figure of £0.96/kg has been used. Waste disposal costs have been estimated at £0.35/L for solvents, which constitute a significant majority of the waste.

3.3 Constraints

This NLP model is relatively small, and it has been implemented in MATLAB. Separate optimisations were performed for temperatures and solvents (25 °C, 45 °C, and 65 °C, and with either toluene or n-hexane). The objective was to minimise the total cost, i.e. the NPV, as calculated by Equation (18):

$$\dot{M}_{pr,API} \geq 100 \tag{27}$$

$$d_{32,sT} < 0.001 \qquad \forall s,T \tag{28}$$

$$V_{t,sT} > 0.0025 \qquad \forall s,T \tag{29}$$

$$0.50 < r_{sT} < 5.00 \qquad \forall s,T \tag{30}$$

$$fsf \geq 1 \tag{31}$$

$$0 \leq x_{ki} \leq 1 \qquad \forall k,i$$

$$\sum_i x_{ki} = 1 \tag{32}$$

The key constraints were target API production (27), the droplet size of the dispersed phase, d_{32}, required for the empirical relations used to be valid (28), a lower bound on key decision variable of LLE vessel (mixer tank) volume (29) to ensure it would not regress to insignificantly small values.

To further keep the problem small and understandable the main decision variable of solvent-to-feed ratio (essentially the mass of solvent per mass of incoming raw feed from the effluent of the third reactor) was restricted from 0.5 to 5.0 by mass (30); the surrogate equations used were derived from data within this range. We have also considered the possibility for flow splits, which implies that we would have a number of parallel LLE vessels (31); naturally, this must be unity or above. Finally, there were of course constraints on mole fractions (32).

The constraint on droplet size, equation (28), can potentially result in a region where the objective function cannot be computed.[35] Foreseeing the potential for algorithms to find local optima as a result of this gap, a global search was performed for the optimisation, where convergence was checked from multiple local starting points; no other local minima were found in the total cost surface, and NLP optimisation results are consistent with our published conceptual ibuprofen CPM separation design.[36]

3.4 Code structure and subroutines

The MATLAB code has a three-tier structure. At the base tier, the physical, chemical and design variables were calculated, encompassing reactor volumes, mass transfer, thermodynamics, and product recovery; equations (4–19) are used in this tier, as well as mass transfer and physical phenomena constraints.

The intermediate tier consisted of cost estimation calculations; equations (1, 3, 20–26) are used here, as well as API production level constraints. This tier calls the base tier, and estimates costs based on the returned variables. Production level constraints are applied at this stage.

The final, top tier applied the nonlinear optimisation, computing the total cost minimisation. In this top tier, some key design space constraints are applied (LLE tank volume V_t, solvent : feed ratio r), and calls the intermediate tier. The solver employed, fmincon, used the default trust-region-reflective method, with tolerances of 10^{-6}. The local solver fmincon was used as there are a variety of non-convexities in the design space, as well as non-continuous regions (where functions can't be evaluated due to the applicability range of empirical equations). To make the problem less computationally demanding to solve, fmincon was used from a variety of starting locations, and the final converged result checked to see if it was the same for all cases; they were, indicating strong results. Gradients were automatically calculated.

3.5 Evaluation of design space

To inform the formulation of the optimisation problem and investigate the design space, the behaviour of the mass transfer coefficient (K), interfacial area (a) and the stage efficiency (E) with varying mixer tank volume (V_t) and solvent-to-feed ratio (r) were investigated. These investigations of the design space, while not the primary focus of this work, illustrate how Quality by Design (QbD) principles can be employed to maximise process potential using systematic evaluation.

Results indicate slightly more pronounced surfaces for K and a in the case of toluene (Figure 11, Figure 12) in comparison to n-hexane (Figure 13, Figure 14). For both solvents, K is promoted by higher rates of solvent use r and tank volume V_t. This is intuitive, as more solvent should among other effects lead to greater concentration driving forces. In contrast, while greater tank volumes also promote interfacial areas between the two immiscible phases, there are significant non-convexities, with a being highest in the region of r = 1 to 1.5 for given tank volumes. It is interesting that we do not obtain the highest specific surface area by driving the solvent to feed ratio to bounds, and there are local optima at intermediate solvent to feed ratios for which we get the maximisation of specific surface area; with respect to tank volume of interfacial area increases monotonically. This is likely due to the empirical nature of the relations used here, and the mechanics of droplet formation and droplet size for given volume fractions.

The LLE stage efficiency E used here has been formally defined by Treybal in the mid-1960s. The behaviour of E was broadly similar for all cases (Figure 15). It is generally high for the range of tank volumes studied, but dropping off significantly with lowest tank volumes and high rates of solvent use, tank volumes lower than 2.5 L were not studied due to this sharp drop off. This is also intuitive, as in these cases it is simply not feasible for sufficient mass transfer to occur in a tank of such a size which would have a small residence time. As long as we do not operate at very low tank volumes suitably high stage efficiencies can be assured, and this observation holds true for all four cases.

There is a faint valley in the design spaces of K, a and E in the case of toluene. A plane of approximately r = 0.6 bisects the surfaces. This is the point demarking where phase inversion occurs. Here, it has been assumed that the phase (aqueous or organic) with the highest mass is the continuous phase, while the other is the discrete phase. Furthermore, it should be noted that while this is indeed an estimation: there is no definite way in which the point of phase inversion, the volume fraction at which the dispersed and continuous phases switch, can be predicted. It is highly dependent on fluid properties, temperature, mixing, and mechanical aspects of the mixer and impeller. Here, it has been assumed that the aqueous phase is dispersed, except at the lowest of solvent-to-feed ratios, where it is unlikely that the aqueous phase remains dispersed. This is the reason for the faint valley seen in Figure 11–Figure 15, at the low end of r.

While not as apparent in the results shown here, in previous work there was an interesting discontinuity in the surfaces for K, a, and E, arising from the maximum permissible dispersed phase droplet size (the Sauter mean diameter, d_{32}).[35] This is visible for the surfaces of n-hexane (Figure 13–Figure 15). Care must always be taken when using empirical relations with defined regions of applicability, as they could lead to local optima.

T = 25 °C

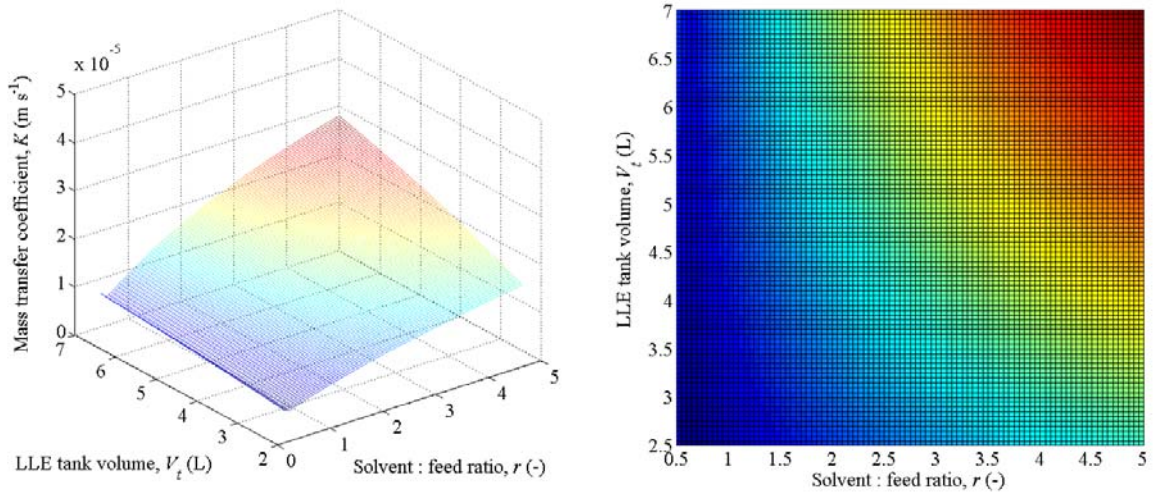

T = 45 °C

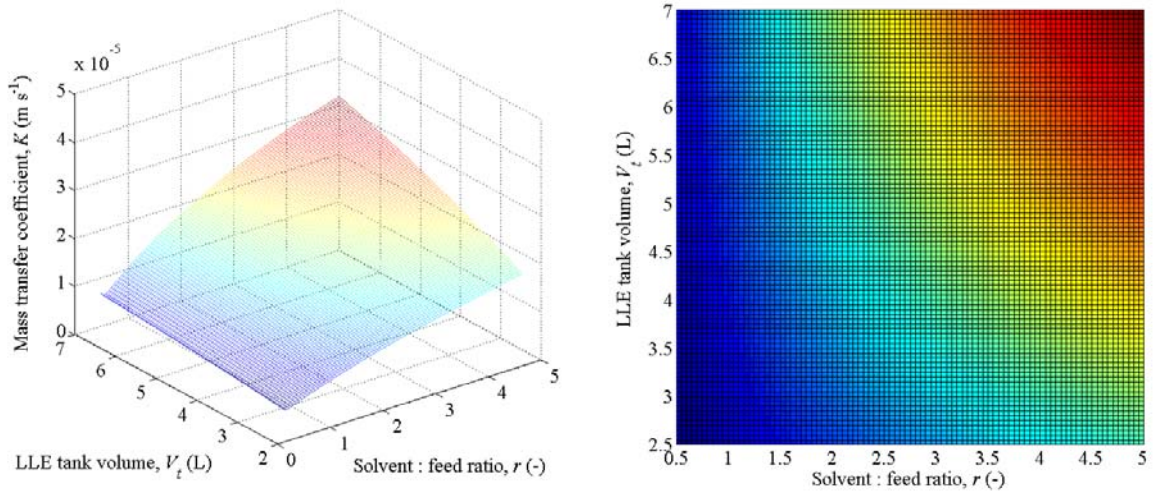

T = 65 °C

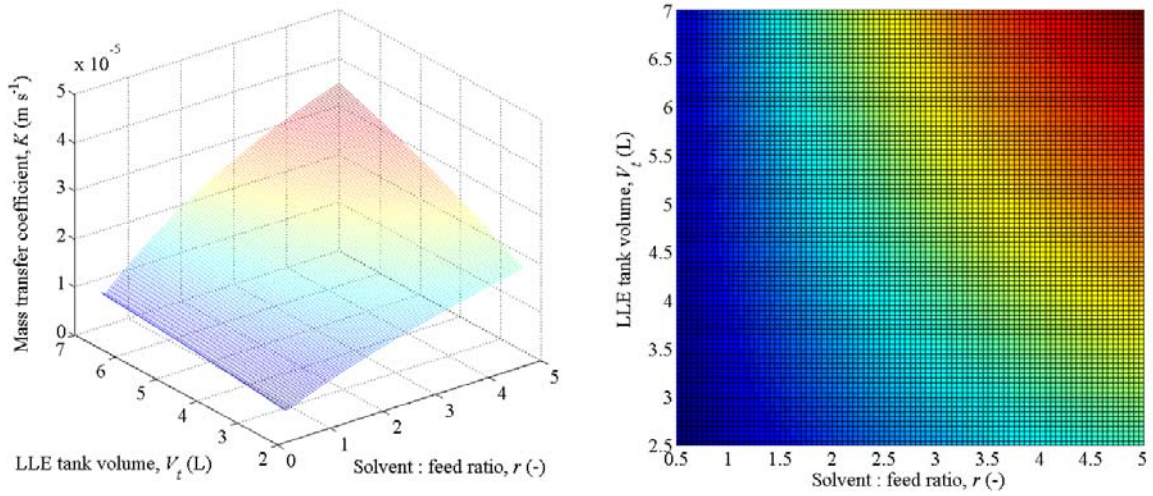

Figure 11. Mass transfer coefficient variation with solvent : feed ratio and LLE tank volume for toluene use.

T = 25 °C

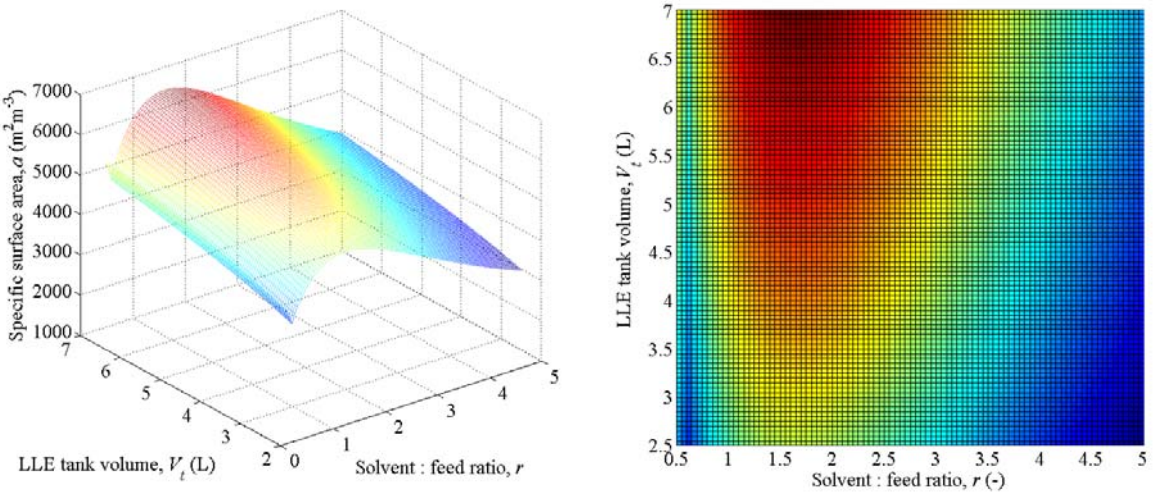

T = 45 °C

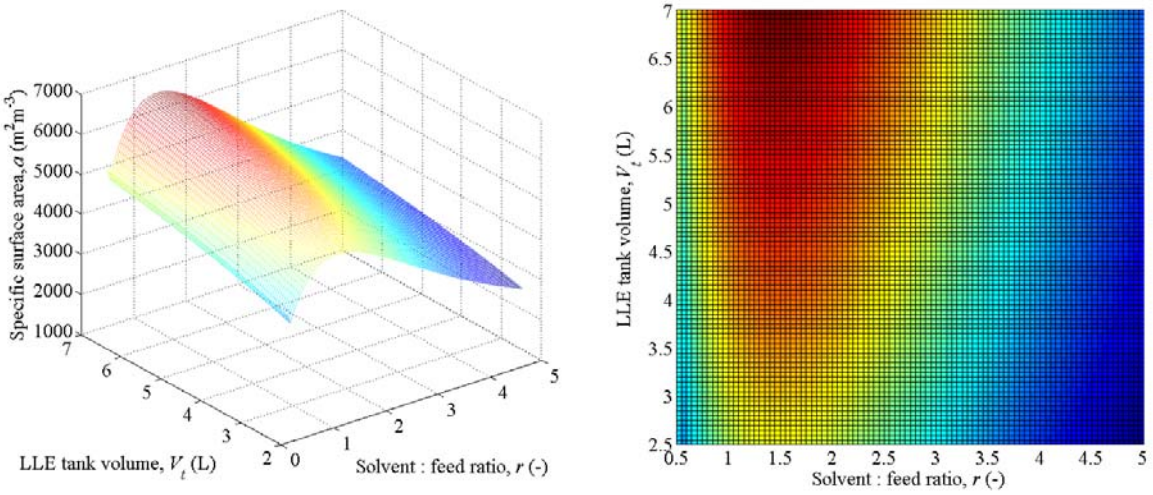

T = 65 °C

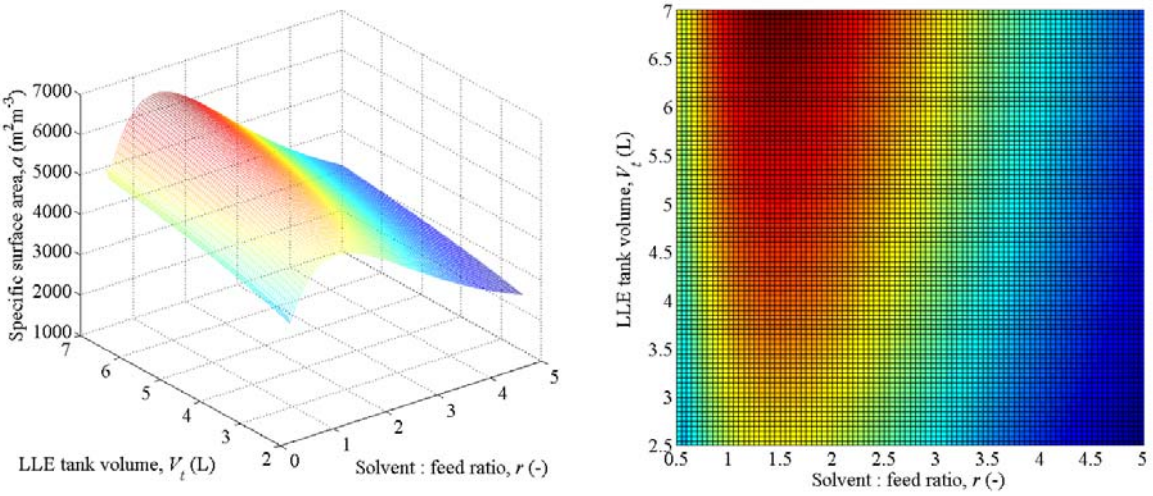

Figure 12. Interfacial area variation with solvent : feed ratio and LLE tank volume for toluene use.

T = 25 °C

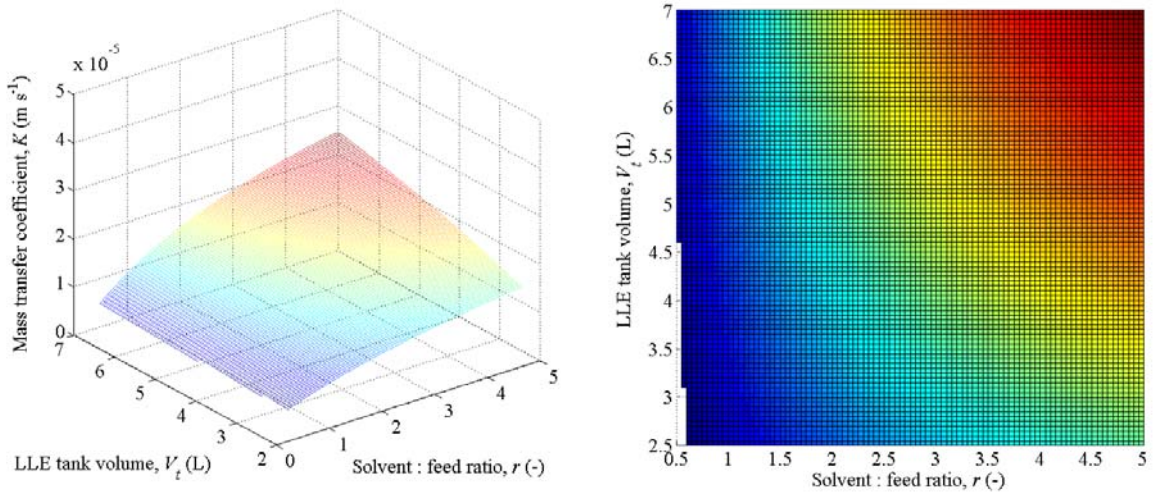

T = 45 °C

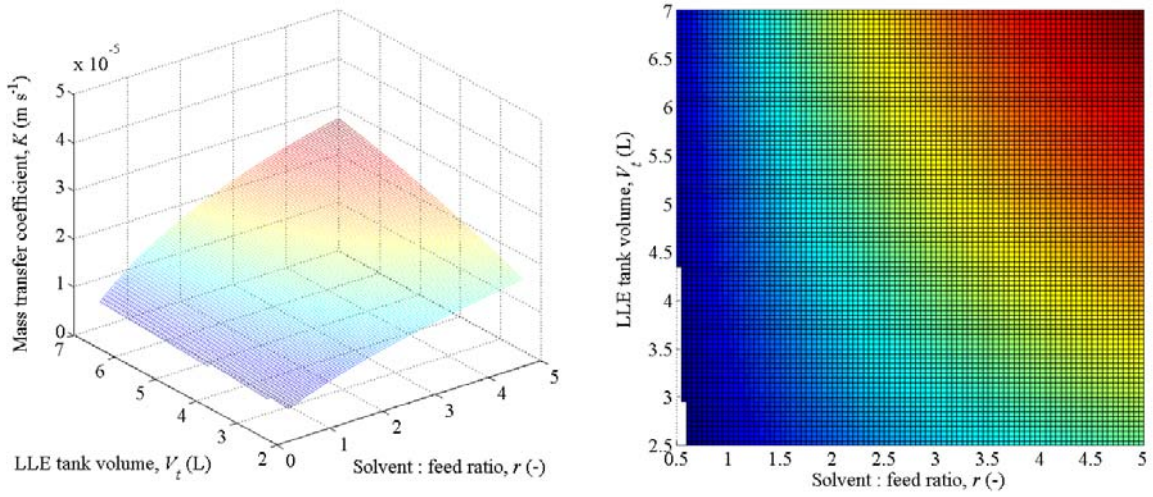

T = 65 °C

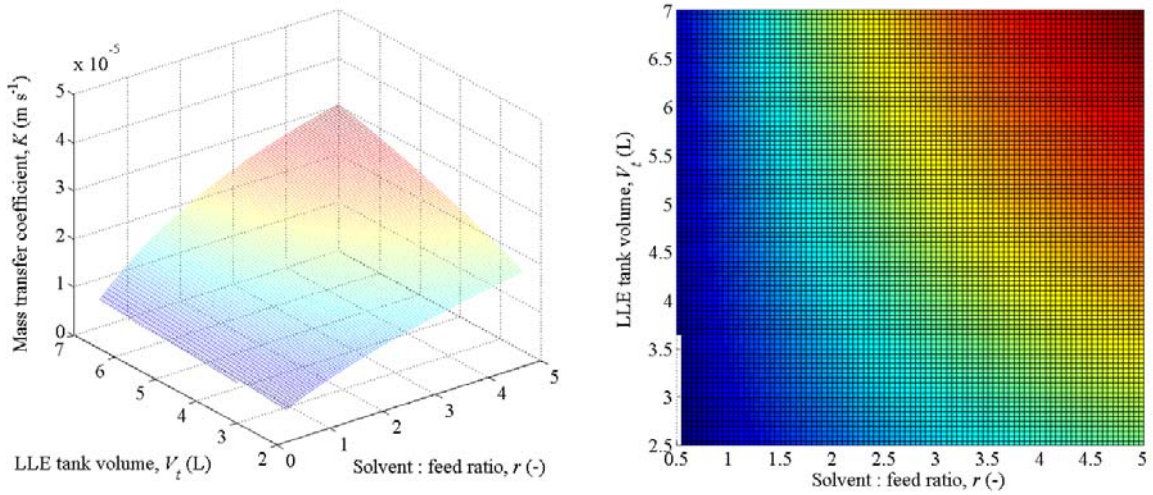

Figure 13. Mass transfer coefficient variation with solvent : feed ratio and LLE tank volume for n-hexane use.

T = 25 °C

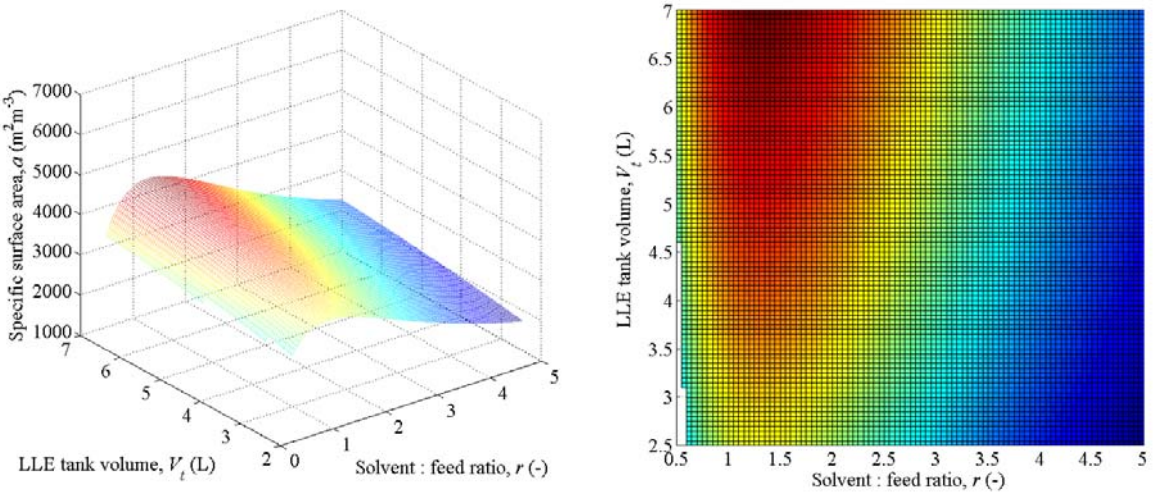

T = 45 °C

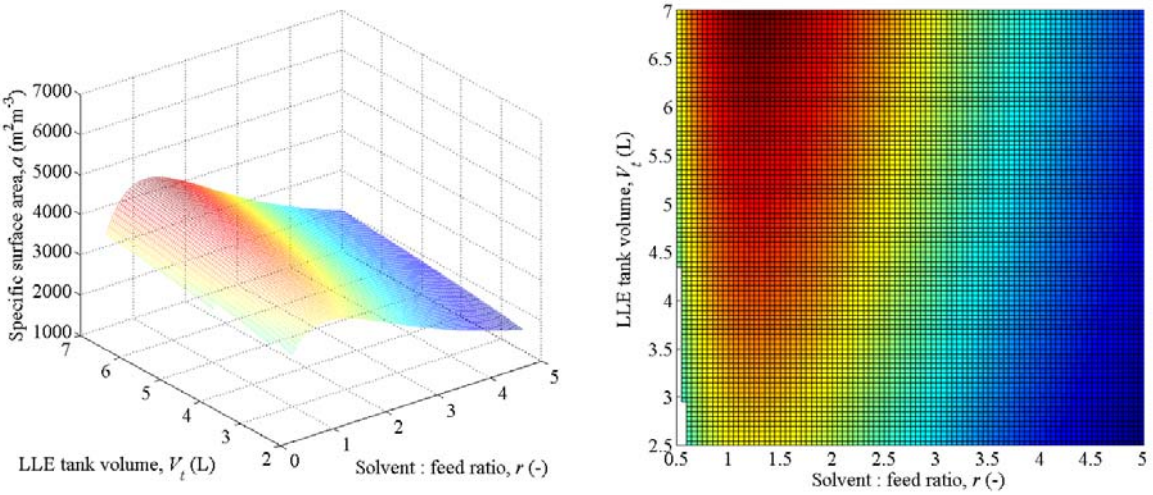

T = 65 °C

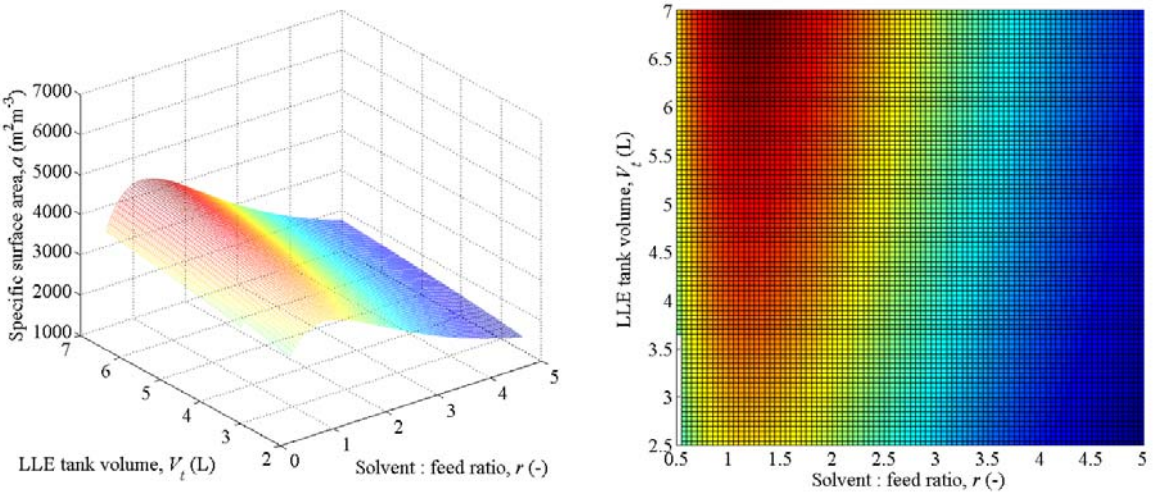

Figure 14. Interfacial area variation with solvent : feed ratio and LLE tank volume for n-hexane use.

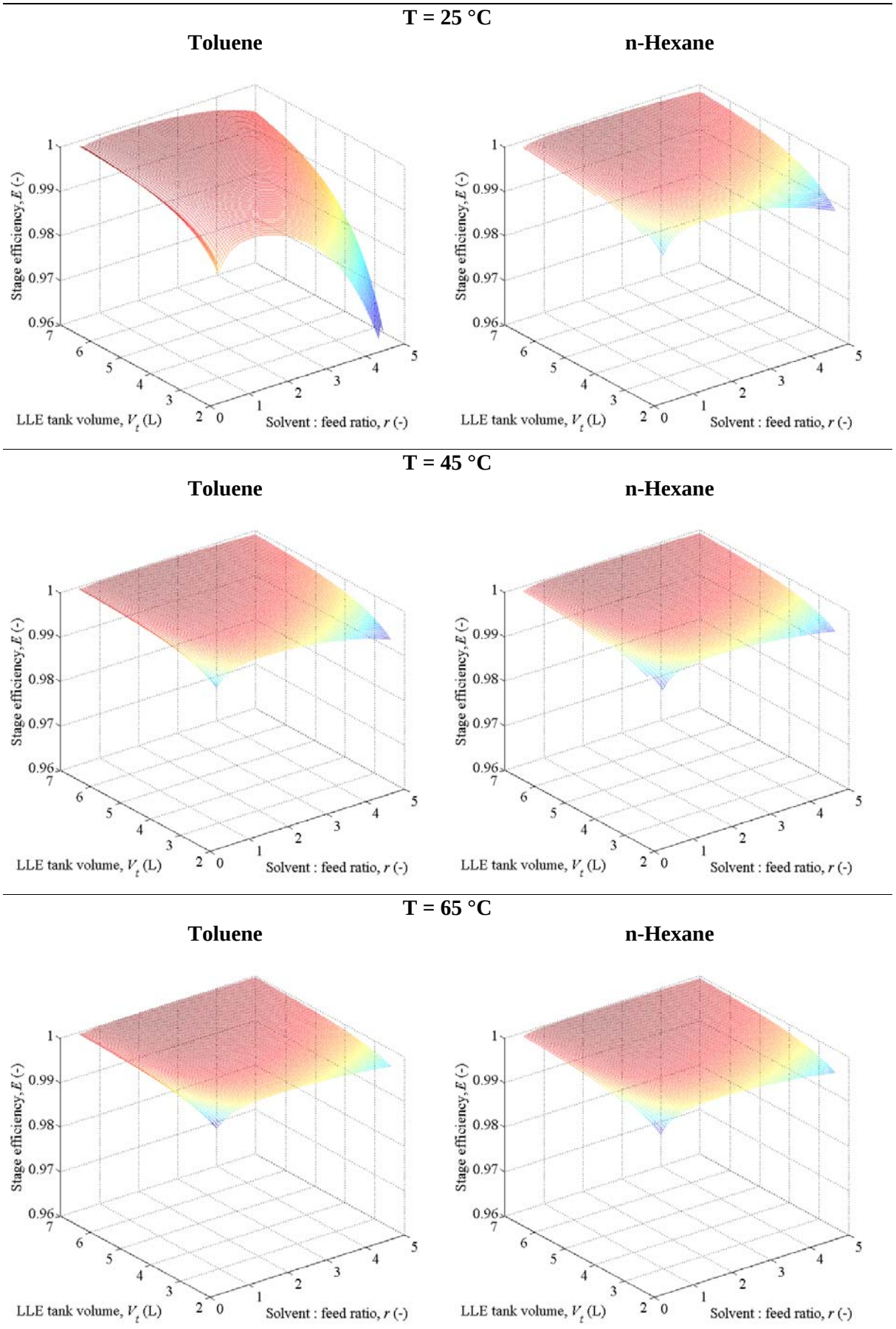

Figure 15. Variation of stage efficiency *E* with tank volume, solvent-to-feed ratio, and temperature.

4 RESULTS AND DISCUSSION

Solution time for each formulation (two solvent cases, each at two temperatures) was generally fast, in the order of 1~10 seconds, due to the concise nature of the formulations. The optimal cost for toluene is 761.4×10^3 GBP, and corresponds to a solvent-to-feed ratio of 0.5, a mixer tank of 4.66 L volume, operating at 65 °C. For n-hexane, the optimal cost is slightly lower at 728.5×10^3 GBP, also for a solvent-to-feed ratio of 0.5, for a mixer tank of 5.70 L, and also operating at 65 °C. This would also beneficial with respect to cooling – there would be no reason to cool the reactor effluent to ambient temperature Detailed views of the optima for each formulation are given in Figure 16 (toluene) and Figure 17 (n-hexane).

A useful and versatile metric for quantifying environmental impact, E-factor has multiple definitions, the simplest of which is the quantity of waste generated per unit of product, in mass terms. Highly efficient industries relying almost completely on continuous production techniques – such as oil and gas – have E-factors in the order of 0.1, while batch-reliant processes such as pharmaceutical production generate significant relative amounts of waste with high E-factors of 200 not uncommon.[37] In this paper, the E-factor is computed where the product is (pure) recovered API, while the waste consists of byproducts (bpd), unconverted reactants (ur), waste solvent (ws, all assumed unrecovered), and unrecovered API (uAPI):

$$E\text{-}factor = \frac{m_{was}}{m_{API}} = \frac{m_{bpd} + m_{ur} + m_{ws} + m_{uAPI}}{m_{API}} \tag{33}$$

There is a consistent trend of lower cost and better (lower) E-factors with increasing temperature for both solvents (Figure 18). For each temperature, n-hexane outperforms toluene. Regarding the total cost surfaces for each case, despite the non-convexities with respect to the design space, there is a much more benign profile (compared to the surfaces of K, a and E) for both toluene and n-hexane at all temperatures. The solvent to feed mass ratio is driven to bounds for toluene; indeed, lower rates of solvent use become unrealistic, requiring significant residence times. We also see that at the higher temperature we obtain both a lower tank volume as well as a lower total cost computed from the model (Figure 16, Figure 17). This makes sense: with the more preferable product API distribution at higher temperatures (Figure 7, Figure 8), a smaller tank is required for the desired performance.

By far the biggest determinant of total cost is the solvent-to-feed ratio (r). In Figure 16 and Figure 17, the axes for r have been restricted to better display the surface trends around the optima; this enhanced resolution also has the effect of making the region where the empirical correlations are inapplicable appear wider than they are (Figure 17). Were the axes not restricted, the effect of r is such that the optima are not clearly visible. There is a large effect from r due to the variation in theoretically possible API product recovery, which is calculated from UNIFAC estimates of its solubility in each phase (Figure 7, Figure 8). At higher values of r, maximum recovery drops, leading to a large increase in process throughput and reactor dimensions if the constraint of 100 kg/year API production is to be satisfied; this is the reason r is pushed to the lower bound of 0.5. Given the low quantities of solvent used in this extraction stage relative to the feed, long residence times will likely be required to ensure adequate inter-phase contact and mass transfer.

There is a trade-off between tank size and rate of inter-phase API mass transfer in the mixer unit. Mass transfer coefficients and interfacial areas both improve with greater mixer tank volume. This effect is even more pronounced in the case of stage efficiency (the amount of API recoverable by the given design of the tank), with it exponentially decreasing with lower tank volumes (Figure 6). This exponential decrease also drastically increases costs, again due to the higher throughput required to meet 100 kg/year of API production.

The ideal number of mixer tanks was always one – it was pushed to bounds. Although this does not of course quantify the added redundancy and flexibility provided by having additional tank, for normal operation, one mixer tank always resulted in the lowest total cost.

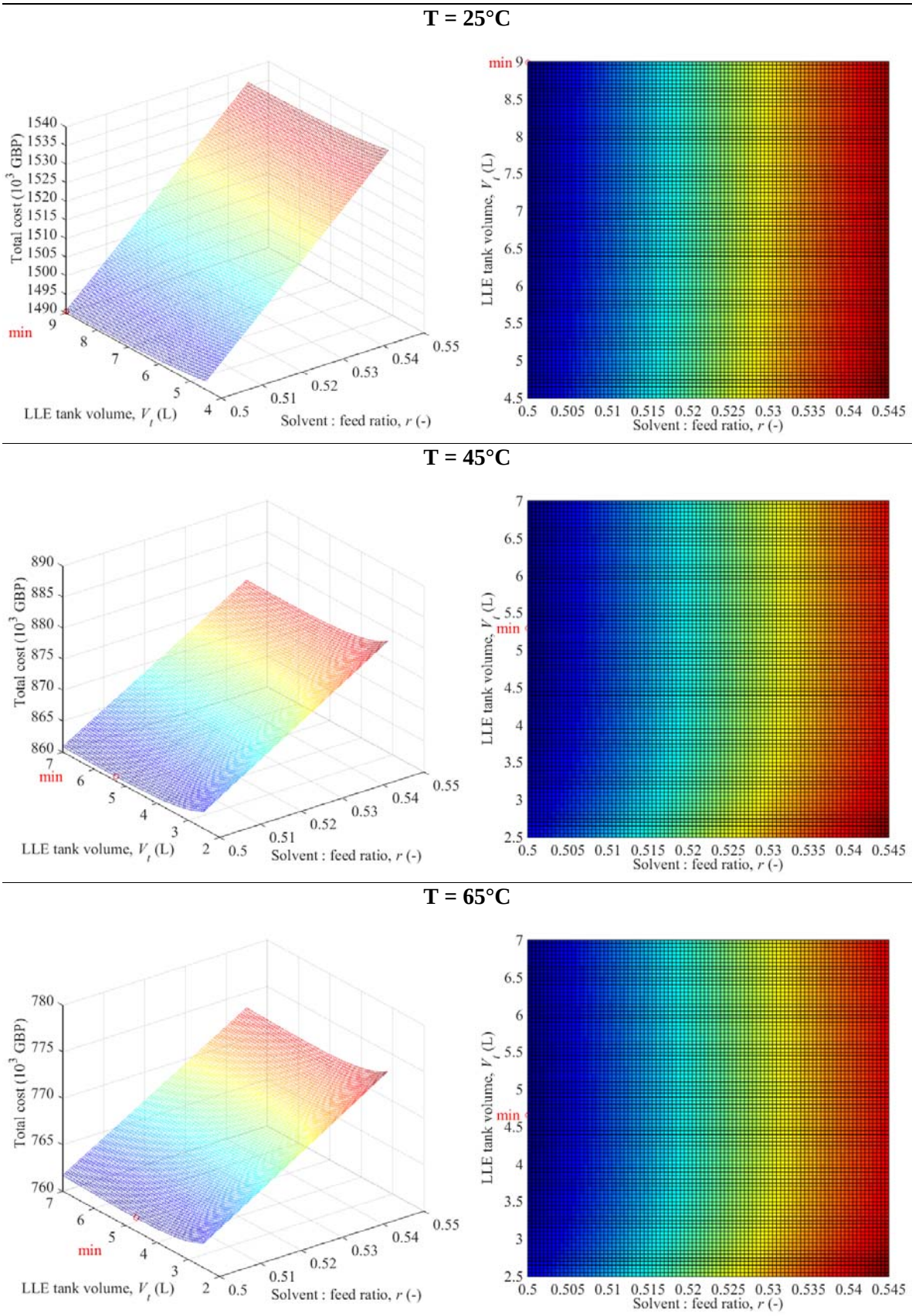

Figure 16. Optima for the use of toluene.

While we compute E-factors and use them to evaluate the potential 'greenness' of the processes, it was not used as an explicit constraint in the optimisation problem. Firstly, in these cases E-factor

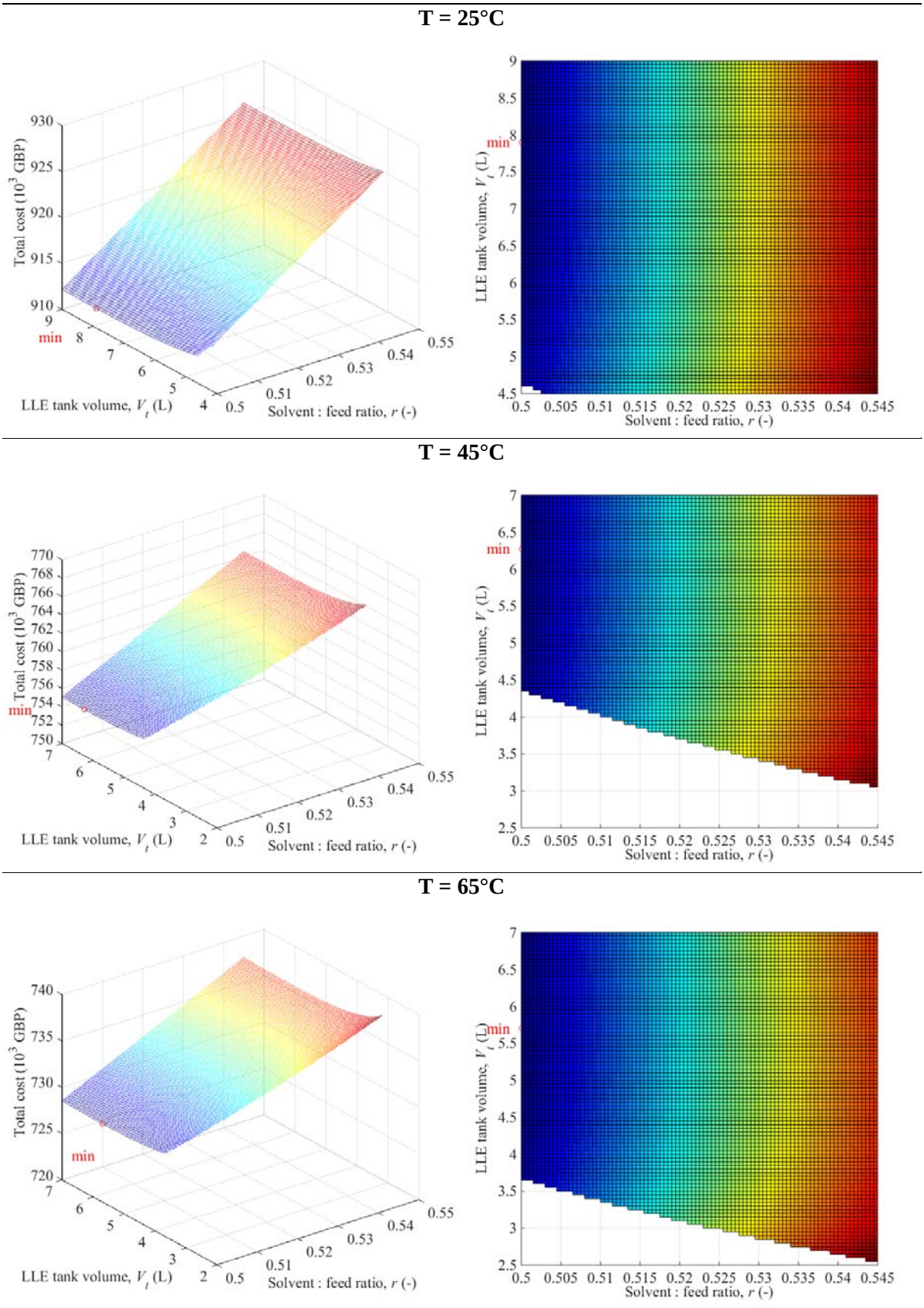

Figure 17. Optima for the use of n-hexane.

performance is already much better with respect to batch manufacturing. The reason that E-factors were not included as explicit constraint was from running the risk of infeasibility due complicated

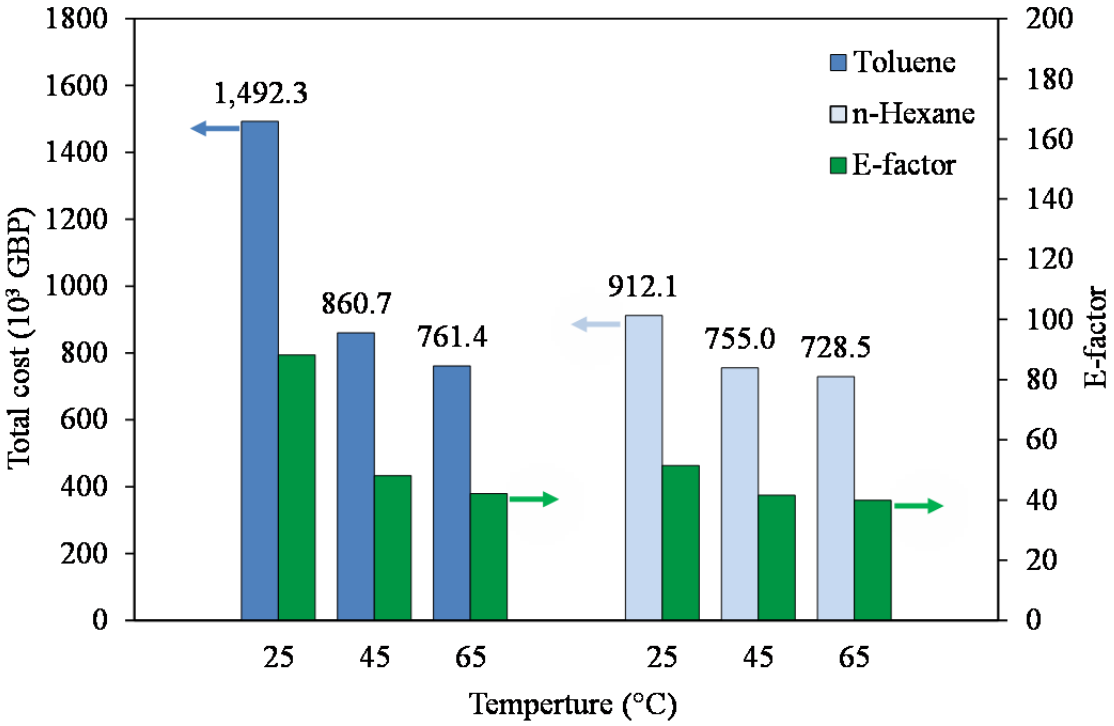

Figure 18. Optimal total costs and E-factors for the six design cases.

thermodynamics and solubilities, even with taking into account the assumptions and simplifications that were made. Although it would indeed be possible to re-cast the problem in a multi-objective framework, with E-factors as a constraint, it is unlikely that feasibility could be ensured while environmental constraints posing strict limits. In such a case a much broader search space would be required, where for example mixed-integer components may be needed for the sake of solving over a much wider set of solvents and an entire spectrum of temperatures. While exhaustive, this would be computationally demanding at this stage.

There is an interesting tradeoff to be made with respect to which case to use. It can be seen that while toluene cost slightly more than n-hexane, and generates more waste (poorer E-factor). While n-hexane would be preferred based on these variables, consideration of other metrics qualify its preferability, and indeed toluene subsequently emerges as the preferred option given that the cost and E-factor differences are small (at 65 °C), and as it is less hazardous compared to n-hexane,[36,37] highlighting how there may be difficult design decisions that are not easily formulated into an optimisation problem.

Summarising, a lowest total cost (728.5×10^3 GBP) is achieved for the case of n-hexane use at 65 °C (Figure 18). The best total cost for toluene, while higher, is only marginally more so at 761.4×10^3 GBP, also at 65 °C. With respect to the E-factor, which qualifies how 'green' the CPM design is, the design cases are comparable apart from toluene a 25 °C, which has a poor E-factor. The best E-factor (39.9) is for the n-hexane at 65 °C, again however the best E-factor for toluene is close at 42.1, also for 65 °C. Given that the differences are small, the use of toluene at 65 °C is the preferable option, considering that it is also more benign than n-hexane. While this value of 42.1 is higher than previously computed cases,[25] the present work employs more accurate thermodynamics and explicit product separation calculations, which results in more conservative but reliable values.

5 CONCLUSIONS

We have formulated and solved a nonlinear programming model for optimisation, as total cost minimisation, of the final separation stage of an upstream continuous flow production process for ibuprofen. The chemistry relies on a continuous synthesis which has been published by Bogdan et al.[6] in 2009.

The design space has been mapped by means of mass transfer correlations which probe liquid-liquid extraction in detail. The most important of the two design variables which we have considered is the solvent to feed ratio, which is the greatest contributor to cost and which has been driven to the lower bound due to the importance of obtaining higher process efficiencies.

High API recoveries are promoted by lower solvent ratios, and the optimal operating temperature is 65 °C for both solvents, where a lowest total cost – 728.5×10^3 GBP – is achieved for the case of n-hexane use, and the lowest total cost for toluene is only marginally higher at 761.4×10^3 GBP. Both solvent options attain respectable E-factor values (39.9 for n-hexane, 42.1 for toluene), and given that the differences are small, the use of toluene at 65 °C is the preferable option, considering that it is also more benign than n-hexane.

6 ACKNOWLEDGMENTS

The authors gratefully acknowledge the financial support of the Engineering and Physical Sciences Research Council (EPSRC) via a Doctoral Training Partnership (DTP) studentship to Mr H.G. Jolliffe.

7 NOMENCLATURE AND ACRONYMS

A'_{sT}	Coefficient used in equation (6)
A_{ipsT}	Coefficient used in equation (5)
API	Active Pharmaceutical Ingredient
a_{sT}	LLE tank specific interfacial surface area using antisolvent *s* at temperature *T*, $m^2\ m^{-3}$
B'_{sT}	Coefficient used in equation (6)
B_{ipsT}	Coefficient used in equation (5)
BLIC	Battery-Limits-Installed-Cost of all equipment in a process, part of CapEx, £
C^*_{sTd}	Equilibrium API concentration of the dispersed phase in the LLE tank
C_{ai}	Reference cost of item *a*, £
CapEx	Capital expenditure, £
C_{con}	Cost of contingency, £
C_{ec}	Factor to account for equipment engineering and construction
c_{fi}	Product of factors that take into account specifics (e.g. material of construction) of item *i*,
C_i	Concentration of species *i*, mol L^{-1}
C_{ins}	Factor to account for equipment installation
C_{ins2}	Factor to account for equipment instrumentation
C_{ipsT}	Coefficient used in equation (5)
C_{mat}	Cost of material raw material purchase (including solvents and catalysts), £
C_{mi0}	Initial concentration of species *i* in PFR *m*, mol L^{-1}
C_{pip}	Factor to account for equipment piping
CPM	Continuous Pharmaceutical Manufacturing
$C_{purc,j}$	Cost of purchase of material *j*, £ kg^{-1}
C_{sTd}	Operating API concentration of the dispersed phase in the LLE tank (also that of the product stream)
C_{utl}	Cost of utilities, £
C_{was}	Cost of waste handling, £
C_{wc}	Cost of working capital, £
d_{32}	Sauter mean droplet diameter, m
$D_{API,c}$	Diffusivity of API in the LLE tank continuous phase, $m^2\ s^{-1}$
$D_{API,d}$	Diffusivity of API in the LLE tank dispersed phase, $m^2\ s^{-1}$
d_i	LLE tank impeller diameter, m
d_t	LLE tank internal diameter, m
E-factor	Environmental factor, a measure of material efficiency, kg (waste)/kg (product API)
Eo	Eotvos number
E_{sT}	LLE tank stage efficiency when using antisolvent *s* at temperature *T*

f_{con}	Factor relating the contingency to the Battery-Limits-Installed-Cost
$FOB_{(Tot)}$	(Total) Free-on-Board cost of equipment
Fr_c	Froude number (LLE tank continuous phase)
fsf	Flow split factor (number of parallel separation processes)
$\dot{f}_{sT}$	Rate of API recovery, mol s^{-1}
f_{utl}	Factor relating the cost of utilities to the total annual requirements (kg) of material
f_{was}	Factor relating the cost of waste handling to the volume of waste
f_{wc}	Factor relating the working capital to the cost of materials
k_b	Boltzmann constant
k_c	LLE tank continuous phase mass transfer coefficient, m s^{-1}
k_d	LLE tank dispersed phase mass transfer coefficient, m s^{-1}
k_i	Rate constant of species i, L mol^{-1} hr^{-1}
K_{sT}	LLE tank overall mass transfer coefficient using antisolvent s at temperature T, m s^{-1}
m_{API}	Mass of API produced after separation, kg yr^{-1}
m_{bpd}	Mass of by-product waste, kg yr^{-1}
$\dot{M}_{pr,API}$	Annual production of API (kg y^{-1})
m_{uAPI}	Mass of unrecovered API, kg yr^{-1}
m_{ur}	Mass of unreacted reagent waste, kg yr^{-1}
m_{was}	Total mass of waste, kg yr^{-1}
m_{ws}	Mass of solvent waste, kg yr^{-1}
N_i	LLE tank impeller rotation speed, rps
NPV	Net Present Value, the total costs over a certain plant lifetime, adjusted to the present
O	Indicates organic phase
$OpEx$	Operating expenditure, £
p_i	Dimensionless exponent used in cost-capacity equation (21)
$\dot{Q}_s$	Volumetric flow through the LLE tank, m^3 s^{-1}
$\dot{Q}_m$	Volumetric flowrate in PFR m, mL hr^{-1}
r	LLE tank antisolvent : feed ratio (kg kg-1)
r_{API}	Molecular radius of ibuprofen, m
Re_i	Impeller Reynolds number
Req_j	Annual requirements of material j, kg y^{-1}
r_i	Reaction rate of molecule i, mol L^{-1} hr^{-1}
$R_{max,sT}$	Theoretical maximum API recovery using antisolvent s at temperature T
S_{ai}	Reference capacity of item i, units depend on item type
S_{bi}	Design capacity of item i, units depend on item type
$Sc_{c/d}$	Schmidt number, continuous (c) or dispersed (d) phase
$Sh_{c/d}$	Sherwood number, continuous (c) or dispersed (d) phase
T	Temperature, °C or K
V_{PFRm}	Volume of plug flor reactor m, mL
V_{tsT}	LLE tank volume using antisolvent s at temperature T, m^3
W	Indicates aqueous phase
We	Weber number
x_{ipsT}	Mole fraction of i in ternary mixture phase p using antisolvent s at temperature T
x_{ki}	Mole fraction of species i in stream k
X_{mi}	Conversion of species i in PFR m
X_{mif}	Final conversion of species i in PFR m
y	Discount rate, the correction factor for adjusting costs to the present
$\dot{v}_{was}$	Annual generation of waste (L y^{-1})
μ_c	LLE tank continuous phase viscosity, Pa s
μ_m	LLE tank mixture viscosity, Pa s
ρ_c	LLE tank continuous phase density, kg m^{-3}
ρ_d	LLE tank dispersed phase density, kg m^{-3}
ρ_m	LLE tank mixture density, kg m^{-3}
σ	LLE tank dispersed phase surface tension, N m^{-1}

τ Plant lifetime, years
φ LLE tank dispersed phase volume fraction

8 LITERATURE REFERENCES

1 Schaber, S. D.; Gerogiorgis, D. I.; Ramachandran, R.; Evans, J. M. B.; Barton, P. I.; and Trout, B. L.; Economic Analysis of Integrated Continuous and Batch Pharmaceutical Manufacturing: a Case Study. *Ind. Eng. Chem. Res.* **2011**, *50*, 10083–10092.

2 Gerogiorgis, D. I.; Jolliffe, H. G. Continuous Pharmaceutical Process Engineering and Economics. *Chimica Oggi - Chemistry Today* **2016**, *33*, 29–32.

3 Jiménez-González, C.; Poechlauer, P.; Broxterman, Q.B.; Yang, B.-S.; am Ende, D.; Baird, J.; Bertsch, C.; Hannah, R.E.; Dell'Orco, P.; Noorman, H.; Yee, S.; Reintjens, R.; Wells, A.; Massonneau, V.; Manley, J. Key Green Engineering Research Areas for Sustainable Manufacturing: a Perspective from Pharmaceutical and Fine Chemicals Manufacturers. *Org. Process Res. Dev*. **2011**, *15*, 900–911.

4 Lee, S.L.; O'Connor, T.F.; Yang, X.; Cruz, C.N.; Chatterjee, S.; Madurawe, R.D.; Moore, C.M.V.; Yu, L.X.; Woodcock, J. Modernizing Pharmaceutical Manufacturing: from Batch to Continuous Production. *J. Pharm. Innov.* **2015**, *10*, 191–199.

5 EFPIA. *The Pharmaceutical Industry in Figures - Key Data 2014*; status report by the European Federation of Pharmaceutical Industries and Associations, 2014.

6 Bogdan, A.R.; Poe, S.L.; Kubis, D.C.; Broadwater, S.J.; McQuade, D.T. The Continuous-Flow Synthesis of Ibuprofen. *Angew. Chem. Int. Ed.* **2009**, *48*, 8547–8550.

7 Hopkin, M.D.; Baxendale, I.R.; Ley, S.V. A Flow-Based Synthesis of Imatinib: the API of Gleevec. *Chem. Commun.* **2010**, *46*, 2450–2452.

8 Kopetzki, D.; Lévesque, F.; Seeberger, P.H. A Continuous-Flow Process for the Synthesis of Artemisinin. *Chem. – Eur. J.* **2013**, *19*, 5450–5456.

9 Heider, P.L.; Born, S.C.; Basak, S.; Benyahia, B.; Lakerveld, R.; Zhang, H.; Hogan, R.; Buchbinder, L.; Wolfe, A.; Mascia, S.; Evans, J.M.B.; Jamison, T.F.; Jensen, K.F. Development of a Multi-Step Synthesis and Workup Sequence for an Integrated, Continuous Manufacturing Process of a Pharmaceutical. *Org. Process Res. Dev.* **2014**, *18*, 402–409.

10 Baxendale, I.R.; Braatz, R.D.; Hodnett, B.K.; Jensen, K.F.; Johnson, M.D.; Sharratt, P.; Sherlock, J.-P.; Florence, A.J. Achieving Continuous Manufacturing: Technologies and Approaches for Synthesis, Workup, and Isolation of Drug Substance. May 20–21, 2014 Continuous Manufacturing Symposium. *J. Pharm. Sci.* **2015**, *104*, 781–791.

11 Rogers, A.; Ierapetritou, M. Challenges and Opportunities in Modeling Pharmaceutical Manufacturing Processes. *Comput. Chem. Eng.* **2015**, *81*, 32–39.

12 Gerogiorgis, D.I.; Barton, P.I.. Steady-State Optimization of a Continuous Pharmaceutical Process. *Comput. Aided Chem. Eng.* **2009**, *27*, 927–932

13 Biegler, L.T.; Grossmann, I.E.,. Retrospective on Optimization. *Comput. Chem. Eng.* **2004**, *28*, 1169–1192.

14 Gernaey, K.V.; Cervera-Padrell, A.E.; Woodley, J.M. A Perspective on PSE in Pharmaceutical Process Development and Innovation. *Comput. Chem. Eng.* **2012**, *42*, 15–29.

15 Escotet-Espinoza, M.S.; Rogers, A.; Ierapetritou, M. Optimization Methodologies for the Production of Pharmaceutical Products. In *Process Simulation and Data Modeling in Solid Oral Drug Development and Manufacture*; Ierapetritou, M.G., Ramachandran, R., Eds.; Methods in Pharmacology and Toxicology. Springer New York; 2016; pp. 281–309.

16 Grom, M.; Stavber, G.; Drnovšek, P.; Likozar, B. Modelling Chemical Kinetics of a Complex Reaction Network of Active Pharmaceutical Ingredient (API) Synthesis with Process Optimization for Benzazepine Heterocyclic Compound. *Chem. Eng. J.* **2016**, *283*, 703–716.

17 Patel, M.P.; Shah, N.; Ashe, R. Robust Optimisation Methodology for the Process Synthesis of Continuous Technologies. *Comput. Aided Chem. Eng.* **2011**, *29*, 351–355.

18 Ott, D.; Kralisch, D.; Denčić, I.; Hessel, V.; Laribi, Y.; Perrichon, P.D.; Berguerand, C.; Kiwi-Minsker, L.; Loeb, P. Life Cycle Analysis within Pharmaceutical Process Optimization and Intensification: Case Study of Active Pharmaceutical Ingredient Production. *ChemSusChem* **2014**, *7*, 3521–3533.

19 Ott, D.; Borukhova, S.; Hessel, V. Life Cycle Assessment of Multi-Step Rufinamide Synthesis – From Isolated Reactions in Batch to Continuous Microreactor Networks. *Green Chem.* **2016**, *18*, 1096–1116.
20 Boukouvala, F.; Ierapetritou, M.G. Surrogate-Based Optimization of Expensive Flowsheet Modeling for Continuous Pharmaceutical Manufacturing. *J. Pharm. Innov.* **2013**, *8*, 131–145.
21 Sen, M.; Rogers, A.; Singh, R.; Chaudhury, A.; John, J.; Ierapetritou, M.G.; Ramachandran, R. Flowsheet Optimization of an Integrated Continuous Purification-Processing Pharmaceutical Manufacturing Operation. *Chem. Eng. Sci.* **2013**, *102*, 56–66
22 Abejón, R.; Garea, A.; Irabien, A. Analysis and Optimization of Continuous Organic Solvent Nanofiltration by Membrane Cascade for Pharmaceutical Separation. *AIChE J.* **2014**, *60*, 931–948.
23 Sato, H.; Watanabe, S.; Takeda, D.; Yano, S.; Doki, N.; Yokota, M.; Shimizu, K. Optimization of a Crystallization Process for Orantinib Active Pharmaceutical Ingredient by Design of Experiment to Control Residual Solvent Amount and Particle Size Distribution. *Org. Process Res. Dev.* **2015**, *19*, 1655–1661.
24 Rogers, A.J.; Inamdar, C.; Ierapetritou, M.G. An Integrated Approach to Simulation of Pharmaceutical Processes for Solid Drug Manufacture. *Ind. Eng. Chem. Res.* **2014**, *53*, 5128–5147.
25 Jolliffe, H.G.; Gerogiorgis, D.I. Process Modelling and Simulation for Continuous Pharmaceutical Manufacturing of Ibuprofen. *Chem. Eng. Res. Des.* **2015**, *97*, 175–191.
26 Hilal, S.H; Karickhoff, S.W. *Verification and validation of the SPARC model*; technical report for U.S. Environmental Protection Agency, EPA/600/R-03/033 (NTIS PB2004-101168), 2003.
27 Hilal, S.H. *Estimation of hydrolysis rate constants of carboxylic acid esters and phosphate ester compounds in aqueous systems from molecular structure by SPARC*; technical report for U.S. Environmental Protection Agency, EPA/600/R-06/105 (NTIS PB2007-100142), 2006.
28 Jolliffe, H.G.; Gerogiorgis, D.I. Process Modelling And Simulation For Continuous Pharmaceutical Manufacturing Of Artemisinin. *Chem. Eng. Res. Des.* **2016**, *112*, 310–325.
29 Jolliffe, H.G.; Gerogiorgis, D.I. Plantwide Design and Economic Evaluation of Two Continuous Pharmaceutical Manufacturing (CPM) Cases: Ibuprofen and Artemisinin. *Comput. Aided Chem. Eng.* **2015**, *37*, 2213–2218.
30 VLE-Calc, Liquid-liquid equilibrium database. http://vle-calc.com/ (accessed: 17-Feb-2016).
31 Gracin, S.; Brinck, T.; Rasmuson, Å.C. Prediction of Solubility of Solid Organic Compounds in Solvents by UNIFAC. *Ind. Eng. Chem. Res.* **2002**, *41*, 5114–5124.
32 Skelland, A.H.P.; Moeti, L.T. Mechanism of Continuous-Phase Mass Transfer in Agitated Liquid-Liquid Systems. *Ind. Eng. Chem. Res.* **1990**, *29*, 2258–2267.
33 Woods, D. R. *Rules of Thumb in Engineering Practice*. WILEY-VCH, 2007.
34 Couper, J. R. *Process Engineering Economics*. Marcel Dekker, Inc., 2003.
35 Jolliffe, H.G.; Gerogiorgis, D.I. Technoeconomic Optimization for Green Continuous Pharmaceutical Manufacturing (CPM) of Analgesics. Presented at the 2015 AIChE Annual Meeting, Salt Lake City, UT, USA, 9 November 2015.
36 Jolliffe, H.G.; Gerogiorgis, D.I. Plantwide Design and Economic Evaluation of two Continuous Pharmaceutical Manufacturing (CPM) Cases: Ibuprofen and Artemisinin. *Comput. Chem. Eng.* **2016**, *91*, 269–288.
37 Ritter, S. K., Reducing Environmental Impact of Organic Synthesis. *Chem Eng News.* **2013**, *91*.
38 Alfonsi, K.; Colberg, J.; Dunn, P.J.; Fevig, T.; Jennings, S.; Johnson, T.A.; Kleine, H.P.; Knight, C.; Nagy, M.A.; Perry, D.A.; Stefaniak, M. Green Chemistry Tools to Influence a Medicinal Chemistry and Research Chemistry Based Organisation. *Green Chem.* **2008**, *10*, 31–36.
39 Henderson, R.K.; Jiménez-González, C.; Constable, D.J.C.; Alston, S.R.; Inglis, G.G.A.; Fisher, G.; Sherwood, J.; Binks, S.P.; Curzons, A.D. Expanding GSK's Solvent Selection Guide – Embedding Sustainability into Solvent Selection Starting at Medicinal Chemistry. *Green Chem.* **2011**, *13*, 854–862.
40 Kralj, J.G.; Sahoo, H.R.; Jensen, K.F. Integrated Continuous Microfluidic Liquid-Liquid Extraction. *Lab Chip* **2007**, *7(2)*, 256–263.

GRAPHICAL ABSTRACT

(WEB-ENHANCED OBJECT)